arXiv:1605.09762v1 [math.NA] 31 May 2016

ENERGY-CONSERVING TIME-DISCRETISATION OF ABSTRACT DYNAMIC PROBLEMS WITH APPLICATIONS IN CONTINUUM MECHANICS OF SOLIDS

Tomáš Roubíček [1,2], Christos G. Panagiotopoulos [3]

[1] *Mathematical Institute, Charles University, Sokolovská 83, CZ-186 75 Praha 8, Czech Republic.*
[2] *Institute of Thermomechanics, Czech Acad. Sci., Dolejškova 5, CZ–182 00 Praha 8, Czech Republic*
[3] *Institute of Applied and Computational Mathematics, Foundation for Research and Technology - Hellas, Nikolaou Plastira 100, Vassilika Vouton, GR-700 13 Heraklion, Crete, Greece*

Abstract. An abstract 2nd-order evolution equation or inclusion is discretised in time in such a way that the energy is conserved at least in qualified cases, typically in the cases when the governing energy is component-wise quadratic or "slightly-perturbed" quadratic. Specific applications in continuum mechanics of solids possibly with various internal variables cover vibrations or waves in linear viscoelastic materials at small strains, coupled with some inelastic processes as plasticity, damage, or phase transformations, and also some surface variants related to contact mechanics. The applicability is illustrated by numerical simulations of vibrations interacting with a frictional contact or waves emitted by an adhesive contact of a 2-dimensional viscoelastic body.

Keywords: standard solids with internal parameters, inertia, inelastic processes, plasticity, damage, evolution variational inequalities, numerical approximation, fractional-step splitting, Crank-Nicolson formula, computational simulations.

Mathematical Subject Classification: 35Q74, 35R45, 37N15, 65K15, 65P99, 74C05, 74H15, 74J99, 74M10, 74N30, 74R05, 90C20.

1 INTRODUCTION

Dynamical effects due to inertia play a prominent role in a lot of application of continuum mechanics, and their interaction with various other processes is of a particular interest. Various nonlinear (possibly activated) processes as plasticity, damage, or phase transformations may thus mutually interact with these dynamical forces.

In computational mechanics, so-called transient versus wave propagation problems (i.e. low-frequency vibrations versus high-frequency waves, respectively) are distinguished and different numerical methods are used especially as far as time discretisation concerns. Here we focus on implicit methods, which are also well fitted with mathematical analysis. It is

well known that the backward Euler (also called backward-difference) scheme serves well for theoretical purposes as the so-called Rothe method (see e.g. [17, Chap.5]) but brings unacceptable artificial numerical attenuation by the inertial term which practically prevents any usage for wave computations even if an extremely small time stepping is used. Henceforth, we focus on discretisation schemes that conserves energy at least at some occasions.

For clarity, we make the exposition of the main ideas on an abstract level by considering the initial-value problem for an evolution system of two equations (or, if Ψ's or Φ are not smooth, inclusions):

$$\mathscr{T}'\ddot{u}+\partial\Psi_1(\dot{u})+\partial_u\Phi(u,z)\ni f(t),\qquad u|_{t=0}=u_0,\quad \dot{u}|_{t=0}=v_0, \tag{1a}$$

$$\partial\Psi_2(\dot{z})+\partial_z\Phi(u,z)\ni g(t),\qquad z|_{t=0}=z_0, \tag{1b}$$

where $\mathscr{T}:H\to\mathbb{R}$, $\Phi:U\times Z\to\mathbb{R}$, $\Psi_1:U\to\mathbb{R}$, and $\Psi_2:Z\to\mathbb{R}$ are the (quadratic) kinetic-energy functional, a stored energy functional, and two dissipation functionals, respectively, and $f:[0,T]\to U^*$ and $g:[0,T]\to Z^*$ are the time-dependent loadings, while $U\subset H=H^*$ and Z are Banach spaces and "∂" denotes the convex subdifferential of the possibly nonsmooth functionals Ψ_i or a partial Gâteaux derivative. If the functional is smooth, then the Gâteaux derivative will be briefly denoted by $(\cdot)'$; it is used for $\mathscr{T}'$ in (1a) which is linear so that we write $\mathscr{T}'\ddot{u}$ instead of $\mathscr{T}'(\ddot{u})$.

For efficient computations of dynamical processes, various integration methods, more sophisticated in comparison with the mentioned backward-Euler one, have been devised by Newmark [18] and further generalized by Hilber, Hughes, and Taylor [15] and then used widely in engineering and computational physics. In fact, for a special choice of parameters, the latter method gives the classical Crank-Nicolson scheme [9] if applied to a transformed system of three 1st-order equations (inclusions)

$$\dot{u}=v\,,\qquad u|_{t=0}=u_0, \tag{2a}$$

$$\mathscr{T}'\dot{v}+\partial\Psi_1(v)+\partial_u\Phi(u,z)\ni f\,,\qquad v|_{t=0}=v_0, \tag{2b}$$

$$\partial\Psi_2(\dot{z})+\partial_z\Phi(u,z)\ni g\,,\qquad z|_{t=0}=z_0, \tag{2c}$$

cf. also e.g. [33]. The Crank-Nicolson scheme was originally devised for heat equation and later used for 2nd-order problems in the form (1), see e.g. [14, Ch.6, Sect.9]. It is different if applied to the dynamical equations transformed into the form (2); then it is sometimes called just a central-difference scheme or generalized midpoint scheme, cf. e.g. [30, Sect. 12.2] or [28, Sect. 1.6], respectively.

If Φ is quadratic, this method conserves energy even after time discretisation. It can be used for Ψ_2 1-homogeneous when the limit passage in the discrete semi-stability developed for the backward Euler scheme in the modern theory of rate-independent processes is suitably modified. This will be done in Section 2. This already allows e.g. for application to visco-elasto-dynamic problems coupled with plasticity at small strains like in [28, Sect. 1.6.1] or [30], as outlined in Section 6.

If Φ is only separately quadratic, one can still combine the above outlined Crank-Nicolson type discretisation with the fractional-step method to obtain a suitably decoupled scheme using two Crank-Nicolson formulas. This will be done in Section 3. In special case, even generalization for potentials which are nonquadratic in u or in z can be devised by using suitably defined differential quotients, which will be done on an abstract level in Section 4.

The resting plan of the paper is to discuss convergence of the devised discretisations under suitable data qualification in Section 5 to outline application in continuum mechanics

of solids under small strains in Section 6, and then, in Section 7, to demonstrate computational efficiency of such discretisations on a 2-dimensional dynamic adhesive Mode-II contact of a visco-elastic body with a rigid obstacle.

2 A CRANK-NICOLSON SCHEME FOR Φ QUADRATIC

Rather for notational simplicity, we consider a time step $\tau > 0$ which do not vary in particular time levels, leading to an equidistant partition of the considered time interval. Let us emphasize that, however, a varying time-step and non-equidistant partitions are easily possible to implement because we will always consider only first-order time differences and one-step formulas. In fact, such a varying time-step can be advantageously used for a certain adaptivity to optimize computational costs.

The backward Euler formula applied to (1) serves well for theoretical purposes even for 2nd-order systems under the name "Rothe method" (cf. e.g. [17, 21]) but it is well known that, due to the artificial numerical attenuation, it practically cannot be used for realistic calculation of wave propagation unless $\tau > 0$ is made extremely small. Many other methods have been devised for dynamical problems. A simple method consists in application of the *Crank-Nicolson formula* [9] to the transformed 1st-order system (2). This results to the system for the triple $(u_\tau^k, v_\tau^k, z_\tau^k)$:

$$\frac{u_\tau^k - u_\tau^{k-1}}{\tau} = v_\tau^{k-1/2}, \qquad u_\tau^0 = u_0, \tag{3a}$$

$$\mathscr{T}'\frac{v_\tau^k - v_\tau^{k-1}}{\tau} + \partial\Psi_1\big(v_\tau^{k-1/2}\big) + \partial_u\Phi\big(u_\tau^{k-1/2}, z_\tau^{k-1/2}\big) \ni f_\tau^k\,, \qquad v_\tau^0 = v_0, \tag{3b}$$

$$\partial\Psi_2\Big(\frac{z_\tau^k - z_\tau^{k-1}}{\tau}\Big) + \partial_z\Phi\big(u_\tau^{k-1/2}, z_\tau^{k-1/2}\big) \ni g_\tau^k\,, \qquad z_\tau^0 = z_0, \tag{3c}$$

$$\text{with the abbreviation } u_\tau^{k-1/2} := \frac{u_\tau^k + u_\tau^{k-1}}{2},\ v_\tau^{k-1/2} := \frac{v_\tau^k + v_\tau^{k-1}}{2},\ z_\tau^{k-1/2} := \frac{z_\tau^k + z_\tau^{k-1}}{2} \tag{3d}$$

to be solved recursively for $k = 1, ..., T/\tau$. The right-hand sides can be taken e.g. as $f_\tau^k := f(k\tau)$, or $f_\tau^k := f((k-\frac12)\tau)$, or $f_\tau^k := \frac12 f(k\tau) + \frac12 f((k-1)\tau)$, or $f_\tau^k := \frac1\tau\int_{(k-1)\tau}^{k\tau} f(t)\,\mathrm{d}t$, and similarly for g_τ^k, the particular choice not being essential for our considerations below. This approximation was suggested in engineering literature for the system without z-variable, i.e. for (3a,b), e.g. in [20, 31, 33], possibly even in a nonlinear variant using a non-centered adaptively tuned formula. Actually, it falls into a broader class of so-called Hilber-Hughes-Taylor formulas widening the popular Newmark method [18] as a special choice of parameters (namely $\alpha = \beta = 1/2$ and $\gamma = 1$ in the usual notation, cf. [15]). To be mentioned here that an extension of the Hilber-Hughes-Taylor method has been presented known as the generalized-α method [6] allowing high frequency energy dissipation with second order accuracy.

This system does not satisfy the usual symmetry condition and thus does not have any potential, but eliminating v_τ^k by substituting $v_\tau^k = \frac{2}{\tau}(u_\tau^k - u_\tau^{k-1}) - v_\tau^{k-1}$ into (3b), one again obtains a potential problem for the couple (u_τ^k, z_τ^k). To be more specific, $(u_\tau^k, z_\tau^k) \in U \times Z$ is a minimizer of the functional

$$\begin{aligned}(u,z) \mapsto \frac{2}{\tau}\Phi\Big(\frac{u+u_\tau^{k-1}}{2}\,,\frac{z+z_\tau^{k-1}}{2}\Big) + \Psi_1\Big(\frac{u-u_\tau^{k-1}}{\tau}\Big) + \Psi_2\Big(\frac{z-z_\tau^{k-1}}{\tau}\Big)\\ + 2\tau\mathscr{T}\Big(\frac{u-\tau v_\tau^{k-1}-u_\tau^{k-1}}{\tau^2}\Big) - \Big\langle f_\tau^k, \frac{u}{\tau}\Big\rangle - \Big\langle g_\tau^k, \frac{z}{\tau}\Big\rangle\,,\end{aligned} \tag{4}$$

and then one simply calculate $v_\tau^k = \frac{2}{\tau}(u_\tau^k - u_\tau^{k-1}) - v_\tau^{k-1} \in H$.

Existence of a potential is thus also advantageous to ensure existence of a solution $(u_\tau^k, v_\tau^k, z_\tau^k) \in U \times H \times Z$ to (3) just by the direct method. In this section, we will assume:

$$\Phi : U \times Z \to \mathbb{R} \ \text{ coercive, quadratic,} \tag{5a}$$

$$\mathscr{T} : H \to \mathbb{R} \ \text{ quadratic, coercive,} \tag{5b}$$

$$\Psi_1 : U \to \mathbb{R} \cup \infty, \ \Psi_2 : Z \to \mathbb{R} \cup \infty \quad \text{convex,}$$
$$\text{lower semicontinuous, } p_i\text{-coercive (i.e. } \Psi_i(\cdot) \geq \epsilon \|\cdot\|^{p_i}). \tag{5c}$$

The coercivity of Φ means that $\lim_{\|u\|\to\infty, \|z\|\to\infty} \Phi(u,z)/(\|u\| + \|z\|) = \infty$ and, in fact, can be weakened if combined with a coercivity of Ψ_1 or Ψ_2. Altogether, the potential in (4) is convex and weakly lower semicontinuous, which ensures the mentioned existence of its minimizer which solves also (3) provided $U \times Z$ is reflexive and

$$f_\tau^k \in U^* \ \text{ and } \ g_\tau^k \in Z^* \ \text{ and } \ (u_0, v_0, z_0) \in U \times H \times Z. \tag{6}$$

By testing (3b) by $v_\tau^k + v_\tau^{k-1}$ and substituting also $v_\tau^k + v_\tau^{k-1} = \frac{2}{\tau}(u_\tau^k - u_\tau^{k-1})$ due to (3a) and by testing (3c) by $z_\tau^k - z_\tau^{k-1}$, after summation we obtain the equality

$$\frac{\mathscr{T}(v_\tau^k) - \mathscr{T}(v_\tau^{k-1})}{\tau} + \Xi_1\big(v_\tau^{k-1/2}\big) + \Xi_2\Big(\frac{z_\tau^k - z_\tau^{k-1}}{\tau}\Big) + \frac{\Phi(u_\tau^k, z_\tau^k) - \Phi(u_\tau^{k-1}, z_\tau^{k-1})}{\tau}$$
$$= \big\langle f_\tau^k, v_\tau^{k-1/2}\big\rangle + \Big\langle g_\tau^k, \frac{z_\tau^k - z_\tau^{k-1}}{\tau}\Big\rangle \tag{7}$$

with the dissipation rates defined by

$$\Xi_1(v) := \big\langle \partial\Psi_1(v), v\big\rangle \quad \text{and} \quad \Xi_2(\dot z) := \big\langle \partial\Psi_1(\dot z), \dot z\big\rangle, \tag{8}$$

and where we used the structural assumption that both $\mathscr{T}$ and Φ are quadratic. More specifically, we used the two following binomial formulas:

$$\mathscr{T}'\frac{v_\tau^k - v_\tau^{k-1}}{\tau} \cdot \frac{v_\tau^k + v_\tau^{k-1}}{2} = \frac{\mathscr{T}(v_\tau^k) - \mathscr{T}(v_\tau^{k-1})}{\tau}, \tag{9a}$$

$$\Phi'_z\Big(\frac{u_\tau^k + u_\tau^{k-1}}{2}, \frac{z_\tau^k + z_\tau^{k-1}}{2}\Big) \cdot \Big(\frac{v_\tau^k + v_\tau^{k-1}}{2}, \frac{z_\tau^k - z_\tau^{k-1}}{\tau}\Big) = \Phi'_z\Big(\frac{u_\tau^k + u_\tau^{k-1}}{2}, \frac{z_\tau^k + z_\tau^{k-1}}{2}\Big) \cdot$$
$$\cdot \Big(\frac{u_\tau^k - u_\tau^{k-1}}{\tau}, \frac{z_\tau^k - z_\tau^{k-1}}{\tau}\Big) = \frac{\Phi(u_\tau^k, z_\tau^k) - \Phi(u_\tau^{k-1}, z_\tau^{k-1})}{\tau}. \tag{9b}$$

In particular as a special case if $\Psi_1 = \Psi_2 = 0$, $f = 0$, and $h = 0$, the equality (7) shows that the discrete scheme (3) conserves the kinetic and stored energy: $\mathscr{T}(v_\tau^k) + \Phi(u_\tau^k, z_\tau^k) = \text{constant}$.

The scheme investigated in this Section 2 covers various linear rheological models (as Kelvin-Voigt's, Maxwell's, Jeffreys', Burgers', etc.) which use the dissipation potentials Ψ's quadratic, i.e. $p_1 = p_2 = 2$, and could be easily implemented numerically [19], cf. also Remark 6.4 below.

The non-quadratic potentials Ψ's, considered above too, allow e.g. for modeling of certain inelastic processes. Even they can be nonsmooth at 0, i.e. these processes may be activated in the sense that their evolution needs the corresponding driving force to achieve a certain threshold. Moreover, some of them can be 1-homogeneous, so that $p_1 = 1$ or $p_2 = 1$, which means that these processes can be rate independent, although the whole system remains rate dependent due to the inertia and possibly also due to the other Ψ-potential.

Although (5a) still brings substantial restriction on generality, various variants of rate-independent linearized plasticity, with kinematic or isotropic hardening, or without hardening (perfect plasticity) or with plastic-strain gradient are thus covered.

Remark 2.1 In fact, in this section the additive splitting $\Psi(\dot u,\dot z)=\Psi_1(\dot u)+\Psi_2(\dot z)$ can easily be avoided and a general coupling of dissipative forces can be considered.

3 FRACTIONAL-STEP SPLITTING OF CRANK-NICOLSON SCHEME

The quadratic (and in particular convex) structure of Φ considered in Section 2 is a severe restriction and excludes interesting applications. In particular, suddenly triggered processes (like rupture) are hard to model. Thus relaxing this structural restriction is highly desirable. This can be achieved by decoupling the time-discretised system suitably, namely "componentwise". This allows to qualify Φ only "componentwise" and works successfully if the dissipation potentials Ψ's are separated, as indeed the case of our system (1). It is called a fractional-step method or sometimes also a Lie-Trotter (or sequential) splitting, and there is an extensive literature about it, cf. [16, 32]. Actually, the Crank-Nicolson scheme itself can be understood as a splitting, cf. [11].

Let us first relax (5a) by assuming that

$$\Phi: U\times Z\to\mathbb{R}\quad\text{coercive},\quad \forall z\in Z:\quad \Phi(\cdot,z):U\to\mathbb{R}\ \text{ quadratic, convex,}\tag{10a}$$

$$\forall u\in U:\quad \Phi(u,\cdot):Z\to\mathbb{R}\ \text{ quadratic, convex,}\tag{10b}$$

while (5b,c) remains unchanged. We now modify (3) as follows:

$$\frac{u_\tau^k-u_\tau^{k-1}}{\tau}=v_\tau^{k-1/2},\qquad u_\tau^0=u_0,\tag{11a}$$

$$\mathscr{T}'\frac{v_\tau^k-v_\tau^{k-1}}{\tau}+\partial\Psi_1\big(v_\tau^{k-1/2}\big)+\partial_u\Phi\big(u_\tau^{k-1/2},z_\tau^{k-1}\big)\ni f_\tau^k,\qquad v_\tau^0=v_0,\tag{11b}$$

$$\partial\Psi_2\Big(\frac{z_\tau^k-z_\tau^{k-1}}{\tau}\Big)+\partial_z\Phi(u_\tau^k,z_\tau^{k-1/2})\ni g_\tau^k,\qquad z_\tau^0=z_0,\tag{11c}$$

where we again use the notation (3d). Note that the system (11) is indeed decoupled: first (11a,b) is to be solved for (u_τ^k,v_τ^k) and then (11c) is to be solved for z_τ^k. Sometimes, this componentwise-split Crank-Nicolson method is also called the second-order Yanenko method [11].

Likewise (4), an algorithmically useful observation is that these problems possess potentials but, in contrast to (3), now two potentials are to be identified, namely

$$u\mapsto\frac{2}{\tau}\Phi\Big(\frac{u+u_\tau^{k-1}}{2},z_\tau^{k-1}\Big)+\Psi_1\Big(\frac{u-u_\tau^{k-1}}{\tau}\Big)+2\tau\mathscr{T}\Big(\frac{u-\tau v_\tau^{k-1}-u_\tau^{k-1}}{\tau^2}\Big)-\Big\langle f_\tau^k,\frac{u}{\tau}\Big\rangle,\tag{12a}$$

$$z\mapsto\frac{2}{\tau}\Phi\Big(u^k,\frac{z+z_\tau^{k-1}}{2}\Big)+\Psi_2\Big(\frac{z-z_\tau^{k-1}}{\tau}\Big)-\Big\langle g_\tau^k,\frac{z}{\tau}\Big\rangle.\tag{12b}$$

Note that, under the assumptions (5b) and (10), both these potentials are convex and coercive, which may algorithmically facilitate numerical solution of (11a,b) and (11c). And, like in Section 2, existence of a solution to (11) is guaranteed by the direct-method arguments provided again (6) holds.

To show energy conservation even in the discrete scheme, we use the same test as we made for (3), namely $v_\tau^{k-1/2}$ for (11b) and $\frac{z_\tau^k - z_\tau^{k-1}}{\tau}$ for (11c). Using (10), it gives

$$\frac{\mathscr{T}(v_\tau^k) - \mathscr{T}(v_\tau^{k-1})}{\tau} + \Xi_1\big(v_\tau^{k-1/2}\big) + \frac{\Phi(u_\tau^k, z_\tau^{k-1}) - \Phi(u_\tau^{k-1}, z_\tau^{k-1})}{\tau} = \big\langle f_\tau^k, v_\tau^{k-1/2}\big\rangle, \tag{13a}$$

$$\Xi_2\Big(\frac{z_\tau^k - z_\tau^{k-1}}{\tau}\Big) + \frac{\Phi(u_\tau^k, z_\tau^k) - \Phi(u_\tau^k, z_\tau^{k-1})}{\tau} = \Big\langle g_\tau^k, \frac{z_\tau^k - z_\tau^{k-1}}{\tau}\Big\rangle. \tag{13b}$$

It is important that the scheme is carefully decoupled in such a way that, when summing (13) up, we benefit from the cancellation of the terms $\pm\Phi(u_\tau^k, z_\tau^{k-1})$ and obtain again the energy equality (7). Here we used together with the binomial formula (9a), other two binomial formulas instead of only one in (9b), namely

$$\begin{aligned}\partial_u\Phi\Big(\frac{u_\tau^k + u_\tau^{k-1}}{2}, z_\tau^{k-1}\Big) \cdot \frac{v_\tau^k + v_\tau^{k-1}}{2} &= \partial_u\Phi\Big(\frac{u_\tau^k + u_\tau^{k-1}}{2}, z_\tau^{k-1}\Big) \cdot \frac{u_\tau^k - u_\tau^{k-1}}{\tau} \\ &= \frac{\Phi(u_\tau^k, z_\tau^{k-1}) - \Phi(u_\tau^{k-1} z_\tau^{k-1})}{\tau}, \quad \text{and} \end{aligned} \tag{14a}$$

$$\partial_z\Phi\Big(u_\tau^k, \frac{z_\tau^k + z_\tau^{k-1}}{2}\Big) \cdot \frac{z_\tau^k - z_\tau^{k-1}}{\tau} = \frac{\Phi(u_\tau^k, z_\tau^k) - \Phi(u_\tau^k, z_\tau^{k-1})}{\tau}. \tag{14b}$$

Remark 3.1 (*More general dissipation.)* Making the dissipation potentials $\Psi_1(\dot u)$ and $\Psi_2(\dot z)$ dependent also on the state (u, z) is easy and widens applications. Then the subdifferentials in (1) and (2) should be only partial with respect to $\dot u$ and $\dot z$ respectively, and the discrete scheme (3b) and (11) should use $\partial_{\dot u}\Psi_1(u_\tau^{k-1}, z_\tau^{k-1}, v_\tau^{k-1/2})$ and $\partial_{\dot z}\Psi_2(u_\tau^{k-1}, z_\tau^{k-1}, \frac{z_\tau^k - z_\tau^{k-1}}{\tau})$ instead of $\partial\Psi_1(v_\tau^{k-1/2})$ and $\partial\Psi_2(\frac{z_\tau^k - z_\tau^{k-1}}{\tau})$, respectively.

4 SPECIAL NONQUADRATIC POTENTIALS Φ

A generalization for nonquadratic cases is very desirable for some applications. Still holding energy-conservation, it can sometimes be realized by a modification of (11b,c) in the spirit of [7, Sec. 3.1] where a specific gradient-flow problem or [3] where a specific compliance contact have been considered. In contrast to e.g. [31], we confine ourselves on such special cases where we will not need any adaptively tuned formula needed iterative implementation. In the abstract case we can assume existence of differential quotients

$$\mathfrak{D}_u\Phi : U \times U \times Z \to U^* \qquad \text{and} \qquad \mathfrak{D}_z\Phi : U \times Z \times Z \to Z^* \tag{15}$$

approximating respectively $\partial_u\Phi$ and $\partial_z\Phi$ in the sense that

$$\forall\, u \in U,\ z \in Z: \qquad \mathfrak{D}_u\Phi(u,u,z) = \partial_u\Phi(u,z) \quad \text{and} \quad \mathfrak{D}_z\Phi(u,z,z) = \partial_z\Phi(u,z)\,, \tag{16a}$$

$$\begin{aligned}\forall\, u, \tilde z \in U,\ z, \tilde z \in Z: \ &\big\langle \mathfrak{D}_u\Phi(u,\tilde u,z), u - \tilde u\big\rangle = \Phi(u,z) - \Phi(\tilde u, z) \quad \text{and} \\ &\big\langle \mathfrak{D}_z\Phi(u,z,\tilde z), z - \tilde z\big\rangle = \Phi(u,z) - \Phi(u,\tilde z),\end{aligned} \tag{16b}$$

$$\mathfrak{D}_u\Phi, \mathfrak{D}_z\Phi \text{ are continuous, and possibly also} \tag{16c}$$

$$\exists\, \mathfrak{F}_{\tilde u, z} : U \to \mathbb{R}: \qquad \mathfrak{D}_u\Phi(u,\tilde u,z) = \partial\mathfrak{F}_{\tilde u,z}(u), \quad \text{and} \tag{16d}$$

$$\exists\, \mathfrak{G}_{u,\tilde z} : Z \to \mathbb{R}: \qquad \mathfrak{D}_z\Phi(u,z,\tilde z) = \partial\mathfrak{G}_{u,\tilde z}(z), \tag{16e}$$

where the continuity assumption (16c) refers to suitable topologies depending on particular situations. Then, omitting now the notation $v_\tau^{k-1/2}$, (11) is to be modified for $k=1,...,T/\tau$ as

$$\frac{u_\tau^k-u_\tau^{k-1}}{\tau}=\frac{v_\tau^k+v_\tau^{k-1}}{2}, \qquad u_\tau^0=u_0, \tag{17a}$$

$$\mathscr{T}'\frac{v_\tau^k-v_\tau^{k-1}}{\tau}+\partial\Psi_1\Big(\frac{u_\tau^k-u_\tau^{k-1}}{\tau}\Big)+\mathfrak{D}_z(u_\tau^k,u_\tau^{k-1},z_\tau^{k-1})\ni f_\tau^k, \qquad v_\tau^0=v_0, \tag{17b}$$

$$\partial\Psi_2\Big(\frac{z_\tau^k-z_\tau^{k-1}}{\tau}\Big)+\mathfrak{D}_z\Phi(u_\tau^k,z_\tau^k,z_\tau^{k-1})\ni g_\tau^k, \qquad z_\tau^0=z_0. \tag{17c}$$

Obviously, (16b) ensures that the test of (17b) and (17c) successively by $\frac{u_\tau^k-u_\tau^{k-1}}{\tau}$ and $\frac{z_\tau^k-z_\tau^{k-1}}{\tau}$ gives again (13) and one can again benefit from cancellation of the "mixed" terms $\pm\Phi(u_\tau^k,z_\tau^{k-1})$ when summing (13) up. In this way, we again obtain the discrete energy conservation (7).

If also (16d,e) holds, two potentials (12) should be modified as

$$u\mapsto\frac{1}{\tau}\mathfrak{F}_{u_\tau^{k-1},z_\tau^{k-1}}(u)+\Psi_1\Big(\frac{u-u_\tau^{k-1}}{\tau}\Big)+2\tau\mathscr{T}\Big(\frac{u-\tau v_\tau^{k-1}-u_\tau^{k-1}}{\tau^2}\Big)-\Big\langle f_\tau^k,\frac{u}{\tau}\Big\rangle, \tag{18a}$$

$$z\mapsto\frac{1}{\tau}\mathfrak{G}_{u_\tau^k,z_\tau^{k-1}}(z)+\Psi_2\Big(\frac{z-z_\tau^{k-1}}{\tau}\Big)-\Big\langle g_\tau^k,\frac{z}{\tau}\Big\rangle. \tag{18b}$$

Existence of such potentials underlying the scheme (17) can in particular cases facilitate numerical solution when appropriate algorithms are used.

This scheme indeed generalizes Sect. 3. Actually, if $\Phi(\cdot,z)$ or $\Phi(u,\cdot)$ are quadratic, one can take simply

$$\mathfrak{D}_u\Phi(u,\tilde u,z):=\partial_z\Phi\Big(\frac{u+\tilde u}{2},z\Big) \quad\text{ or }\quad \mathfrak{D}_z\Phi(u,z,\tilde z):=\partial_z\Phi\Big(u,\frac{z+\tilde z}{2}\Big) \tag{19}$$

so that (17b) or (17c) coincide with (11c), respectively. Then also $\mathfrak{F}_{\tilde u,z}$ and $\mathfrak{G}_{u,\tilde z}$ from (16d,e) exist and can be taken as

$$\mathfrak{F}_{\tilde u,z}(u)=2\Phi\Big(\frac{u+\tilde u}{2},z\Big) \qquad\text{and}\qquad \mathfrak{G}_{u,\tilde z}(z)=2\Phi\Big(u,\frac{z+\tilde z}{2}\Big). \tag{20}$$

In a general non-quadratic $\Phi(\cdot,z)$ or $\Phi(u,\cdot)$, existence of $\mathfrak{D}_u\Phi$ or $\mathfrak{D}_z\Phi$ satisfying (16) however relies rather on a special local scalar character of involved operators, cf. the example (45) below.

Remark 4.1 (*More fractional steps.*) The fractional-step splitting can easily be iterated and the canceling effect is then "telescopic", cf. [21, Rem. 8.25]. Thus some other equations can be easily added. In particular, the heat-transfer problem can be considered to get a 3-step decoupled scheme, cf. [22].

5 CONVERGENCE ANALYSIS IN PARTICULAR CASES

Beside the standard notation for the Lebesgue L^p-spaces, we will use $W^{k,p}$ for Sobolev spaces whose k-th derivatives are in L^p-spaces. We abbreviate $H^k=W^{k,2}$. We consider a fixed time

interval $I=[0,T]$ and, for a Banach space X, we denote by $L^p(I;X)$ the standard Bochner space of Bochner-measurable mappings $I\to X$ with whose norm in X is in $L^p(I)$. Also, $W^{k,p}(I;X)$ denotes the Banach space of mappings from $L^p(I;X)$ whose k-th distributional derivative in time is also in $L^p(I;X)$. Also, $C(I;X)$ and $C_{\rm weak}(I;X)$ will denote the Banach space of continuous and weakly continuous mappings $I\to X$, respectively. Moreover, we denote by $\mathrm{BV}(I;X)$ the Banach space of the mappings $I\to X$ that have bounded variation on I, and by $\mathrm{B}(I;X)$ the space of Bochner measurable, everywhere defined, and bounded mappings $I\to X$. By $\mathrm{Meas}(I;X)$ we denote the space of X-valued measures on I.

First, we define suitably a weak solution to (2). Assuming Φ smooth and using just the definition of the convex subdifferentials $\partial\Psi_1$ and $\partial\Psi_2$, the inclusions in (2b,c) read as

$$\forall\,\tilde v\in U:\qquad \Psi_1(v)\le\Psi_1(\tilde v)+\big\langle f-\partial_u\Phi(u,z)-\mathscr{T}'\dot v\,,\,\tilde v-v\big\rangle, \tag{21a}$$

$$\forall\,\tilde z\in Z:\qquad \Psi_2(\dot z)\le\Psi_2(\tilde z)+\big\langle g-\partial_z\Phi(u,z)\,,\,\tilde z-\dot z\big\rangle\,. \tag{21b}$$

Summing them and integrating over the time interval $I=[0,T]$, using (2a) while making also the calculus $\langle\mathscr{T}'\dot v,\dot u\rangle=\langle\mathscr{T}'\dot v,v\rangle=\langle\mathscr{T}'v,\dot v\rangle=\frac{\rm d}{{\rm d}t}\mathscr{T}(v)$ and $\langle\partial_u\Phi(u,z),\dot u\rangle+\langle\partial_z\Phi(u,z),\dot z\rangle=\frac{\rm d}{{\rm d}t}\Phi(u,z)$, we eventually obtain:

Definition 5.1 (Weak solution.) *We call the triple $u\in W^{1,p_1}(I;U)$, $v\in L^{p_1}(I;U)\cap C_{\rm weak}(I;H)\cap W^{1,1}(I;U^*)$, and $z\in W^{1,p_2}(I;Z)$ a weak solution to* (2) *if*

$$\dot u=v\quad\text{in the sense of distributions, and} \tag{22a}$$

$$\begin{aligned}\int_0^T\Psi_1(\tilde v)+\Psi_2(\tilde z)+\big\langle\mathscr{T}'\dot v+\partial_u\Phi(u,z)-f,\tilde v\big\rangle+\big\langle\partial_z\Phi(u,z)-g,\tilde z\big\rangle+\big\langle f,\dot u\big\rangle+\big\langle g,\dot z\big\rangle\,{\rm d}t\\ +\mathscr{T}(v_0)+\Phi(u_0,z_0)\ge\mathscr{T}(v(T))+\Phi(u(T),z(T))+\int_0^T\Psi_1(\dot u)+\Psi_2(\dot z)\,{\rm d}t\end{aligned} \tag{22b}$$

holds for all $\tilde v\in L^\infty(I;U)$ and $\tilde z\in L^\infty(I;Z)$.

Considering a fixed time step $\tau>0$ as in the previous sections such that T/τ is integer, and $\{u_\tau^k\}_{k=0,\dots,K}$ with $K=T/\tau$, we introduce a notation for the piecewise-constant and the piecewise affine interpolants defined respectively by

$$\overline{u}_\tau(t)=u_\tau^k,\qquad \underline{u}_\tau(t)=u_\tau^{k-1},\qquad \overline{\underline{u}}_\tau(t)=u_\tau^{k-1/2},\qquad\text{and} \tag{23a}$$

$$u_\tau(t)=\frac{t-(k-1)\tau}{\tau}u_\tau^k+\frac{k\tau-t}{\tau}u_\tau^{k-1}\qquad\text{for }(k-1)\tau<t\le k\tau. \tag{23b}$$

Similar meaning has also v_τ, $\overline{v}_\tau$, etc.

First, let us investigate the situation in Section 2, relying on the structural assumption (5) except that the p-homogeneity will not be particularly exploited. In terms of the above introduced interpolants, one can write the scheme (3) analogously to (2) as

$$\dot u_\tau=\overline{\underline{v}}_\tau,\qquad u_\tau\big|_{t=0}=u_0, \tag{24a}$$

$$\mathscr{T}'\dot v_\tau+\partial\Psi_1(\dot u_\tau)+\partial_u\Phi(\overline{\underline{u}}_\tau,\overline{\underline{z}}_\tau)=\overline{f}_\tau,\qquad v_\tau\big|_{t=0}=v_0, \tag{24b}$$

$$\partial\Psi_2(\dot z_\tau)+\partial_z\Phi(\overline{\underline{u}}_\tau,\overline{\underline{z}}_\tau)=\overline{g}_\tau,\qquad z_\tau\big|_{t=0}=z_0, \tag{24c}$$

considered on the time interval $I=[0,T]$. Assuming Ψ_i are convex, cf. (5b), and Φ smooth, the definition of the convex subdifferentials $\partial\Psi_1$ and $\partial\Psi_2$ allows for writing (24) in sum as

the variational inequality

$$\begin{aligned}\big\langle \mathscr{I}'\dot v_\tau + \partial_u\Phi(\underline{u}_\tau,\underline{z}_\tau) - \overline{f}_\tau, \tilde u - \dot u_\tau\big\rangle + \Psi_1(\tilde u)\\ + \big\langle \partial_z\Phi(\underline{u}_\tau,\underline{z}_\tau) - \overline{g}_\tau, \tilde z - \dot z_\tau\big\rangle + \Psi_2(\tilde z) \ge \Psi_1(\dot u_\tau) + \Psi_2(\dot z_\tau)\end{aligned} \tag{25}$$

to hold for any $(\tilde u,\tilde z)\in U\times Z$ and for a.a. $t\in I$. We further use the binomial formulas (9) after summation for $k=1,...,T/\tau$ written in the form

$$\begin{aligned}\int_0^T \big\langle \mathscr{I}'\dot v_\tau + \partial_u\Phi(\overline{\underline{u}}_\tau,\overline{\underline{z}}_\tau),\dot u_\tau\big\rangle + \big\langle \partial_z\Phi(\overline{\underline{u}}_\tau,\overline{\underline{z}}_\tau),\dot z_\tau\big\rangle\,\mathrm{d}t\\ = \mathscr{I}(v_\tau(T)) + \Phi(u_\tau(T),z_\tau(T)) - \mathscr{I}(v_0) - \Phi(u_0,z_0).\end{aligned} \tag{26}$$

Substituting it into (25) integrated over I, we obtain the discrete analog of (22b), namely

$$\begin{aligned}\int_0^T\Big(\Psi_1(\tilde v) + \Psi_2(\tilde z) + \big\langle \mathscr{I}'\dot v_\tau + \partial_u\Phi(\underline{u}_\tau,\underline{z}_\tau) - \overline{f}_\tau,\tilde v\big\rangle + \big\langle \partial_z\Phi(\underline{u}_\tau,\underline{z}_\tau) - \overline{g}_\tau,\tilde z\big\rangle\\ + \big\langle \overline{f}_\tau,\dot u_\tau\big\rangle + \big\langle \overline{g}_\tau,\dot z_\tau\big\rangle\Big)\,\mathrm{d}t + \mathscr{I}(v_0) + \Phi(u_0,z_0)\\ \ge \mathscr{I}(v_\tau(T)) + \Phi(u_\tau(T),z_\tau(T)) + \int_0^T \Psi_1(\dot u_\tau) + \Psi_2(\dot z_\tau)\,\mathrm{d}t,\end{aligned} \tag{27}$$

while an analog of (22a) is just (24a).

In terms of these interpolants, the discrete energy conservation (7) summed for $k=1,...,T/\tau$ can be written as:

$$\begin{aligned}\mathscr{I}(v_\tau(T)) + \Phi(u_\tau(T),z_\tau(T)) + \int_0^T \Xi_1(\overline{\underline{v}}_\tau) + \Xi_2(\dot z_\tau)\,\mathrm{d}t\\ = \mathscr{I}(v_0) + \Phi(u_0,z_0) + \int_0^T \big\langle \overline{f}_\tau,\dot u_\tau\big\rangle + \big\langle \overline{g}_\tau,\dot z_\tau\big\rangle\,\mathrm{d}t\,.\end{aligned} \tag{28}$$

Note however that neither $\overline{v}_\tau$ not $\underline{v}_\tau$ is the velocity corresponding to u_τ, i.e. $\overline{v}_\tau\neq\dot u_\tau$ and $\underline{v}_\tau\neq\dot u_\tau$ in general, although in the limit both $\overline{v}_\tau-\dot u_\tau\to 0$ and $\underline{v}_\tau-\dot u_\tau\to 0$ for $\tau\to 0$. If $v_0\in H\backslash U$, then even both $\overline{v}_\tau$ and $\underline{v}_\tau$ are not valued in U, although $\overline{\underline{v}}_\tau\in L^\infty(I;U)$. In particular, the relation $\dot u_\tau=\overline{\underline{v}}_\tau$ must be taken into account as a vital ingredient accompanied the variational inequality (26).

Proposition 5.2 (Numerical stability of (3) and convergence.) *Let U and Z be reflexive Banach spaces, U densely embedded into a a Hilbert space H, (5) hold, and furthermore $\|\partial\Psi_1(\cdot)\|_{U^*}\le C(1+\|\cdot\|_U^{p_1-1})$ with some $C\in\mathbb{R}$, and let $u_0\in U$, $v_0\in H$, $z_0\in Z$, $f\in L^{p_1'}(I;U^*)+L^1(I;H)$, and $g\in L^{p_2'}(I;Z^*)$ with $p_i'=p_i/(p_i-1)$ with $p_i>1$ from (5c). Then the following a-priori estimates hold:*

$$\|u_\tau\|_{L^\infty(I;U)\cap W^{1,\infty}(I;H)\cap W^{1,p_1}(I;U)}\le C,\qquad \|z_\tau\|_{W^{1,p_2}(I;Z)}\le C, \tag{29a}$$

$$\|\overline{\underline{v}}_\tau\|_{L^\infty(I;H)\cap L^{p_1}(I;U)}\le C,\qquad \|v_\tau\|_{W^{1,\max(p_1',2)}(I;U^*)+W^{1,1}(I;H)}\le C\,. \tag{29b}$$

Moreover, the sequence $(u_\tau,\overline{\underline{v}}_\tau,z_\tau)$ converges weakly in the topologies indicated by the first three estimates (29) to the unique weak solution (u,v,z) due to Definition 5.1. Moreover, if the Banach space U and the potential Ψ_1 (resp. Z and Ψ_2) are uniformly convex and if $p_1\le 2$, we have even the strong convergences*

$$u_\tau\to u \quad \text{in } W^{1,p_1}(I;U),\quad \text{resp.} \tag{30a}$$

$$z_\tau\to z \quad \text{in } W^{1,p_2}(I;Z). \tag{30b}$$

Proof. The first three a-priori estimates in (29) can be obtained by usual estimation from (7), using the Young and the discrete Gronwall inequalities. Then, from (24) by comparison, we obtain also the last estimate in (29b).

Next, by the Banach selection principle, we choose a weakly* convergent subsequence with respect to the weak* topologies in the spaces indicated in the first three a-priori estimates in (29). Having relevant L^∞-estimates at disposal together with corresponding time derivatives estimated, we can also rely on

$$u_\tau(T)\to u(T)\ \text{ in }\ U,\qquad v_\tau(T)\to v(T)\ \text{ in }\ H,\qquad z_\tau(T)\to z(T)\ \text{ in }\ Z\ \text{ weakly.}$$

Then the limit passage from (27) to (22) is easy when exploiting the assumed convexity which makes the right-hand side of (27) weakly lower-semicontinuous and when realizing the assumption (5a) which makes both $\partial_u\Phi$ and $\partial_z\Phi$ linear so that the right-hand side of (27) is weakly continuous. Moreover, passing to the limit in the relation $\dot u_\tau=\underline{\overline{v}}_\tau$ yields $\dot u=v$.

In fact, not only the selected subsequence but even the whole sequence converges to the weak solution (u,v,z) because it is unique. To see this uniqueness, we subtract the equation (inequality) for two solutions and test it by the difference of time derivatives of them. The monotonicity of $\partial\Psi_1$ and $\partial\Psi_2$ is then to be used together with linearity of Φ' and $\mathscr{T}'$; cf. e.g. [21, Prop. 11.35].

The strong convergence (30) can then be seen by estimation:

$$\begin{aligned}
&\int_0^T\Xi_1(v)+\Xi_2(\dot z)\,\mathrm{d}t\le\liminf_{\tau\to0}\int_0^T\Xi_1(\underline{\overline{v}}_\tau)+\Xi_2(\dot z_\tau)\,\mathrm{d}t\le\limsup_{\tau\to0}\int_0^T\Xi_1(\underline{\overline{v}}_\tau)+\Xi_2(\dot z_\tau)\,\mathrm{d}t\\
&\quad=\lim_{\tau\to0}\left(\mathscr{T}(v_0)+\Phi(u_0,z_0)+\int_0^T\big\langle\overline{f}_\tau,\underline{\overline{v}}_\tau\big\rangle+\big\langle\overline{g}_\tau,\dot z_\tau\big\rangle\,\mathrm{d}t-\mathscr{T}(v_\tau(T))-\Phi(u_\tau(T),z_\tau(T))\right)\\
&\quad\le\mathscr{T}(v_0)+\Phi(u_0,z_0)+\int_0^T\big\langle f,v\big\rangle+\big\langle g,\dot z\big\rangle\,\mathrm{d}t-\mathscr{T}(v(T))-\Phi(u(T),z(T))\\
&\quad=\int_0^T\Xi_1(v)+\Xi_2(\dot z)\,\mathrm{d}t
\end{aligned}\tag{31}$$

where the first equality has used (28) while the last equality is based on that (2) is already proved together with the fact that $\dot v\in L^{\max(p_1',2)}(I;U^*)+L^1(I;H)$ is in duality with $v\in L^{p_1}(I;U)\cap L^\infty(I;H)$ so that the by-part integration of the $\mathscr{T}$-term can legally be executed; here we needed $p_1\le2$. Note that $\dot v$ indeed remains in the nonreflexive space $L^{\max(p_1',2)}(I;U^*)+L^1(I;H)$ by a comparison argument because $f-\partial\Psi_1(v)-\partial\Phi(u,z)$ is in this space. Similarly, we use the estimates on $\dot u$ and $\dot z$ for the by-part integration of the Φ-term; note that $\dot u\in L^\infty(I;H)\cap L^{p_1}(I;U)$ is certainly in duality with $\partial_u\Phi(u,z)\in L^\infty(I;U^*)$ and $\dot z\in L^{p_2}(I;Z)$ in duality with $\partial_z\Phi(u,z)\in L^\infty(I;Z^*)$. Therefore, (31) implies that

$$\lim_{\tau\to0}\int_0^T\Xi_1(\underline{\overline{v}}_\tau)+\Xi_2(\dot z_\tau)\,\mathrm{d}t=\int_0^T\Xi_1(v)+\Xi_2(\dot z)\,\mathrm{d}t.\tag{32}$$

The assumed uniform convexity of Ψ's and of the underlying Banach spaces U and Z (and thus of $L^{p_1}(I;U)$ and $L^{p_2}(I;Z)$ too) together with the weak convergence then yields the strong convergence (30) by the Fan-Glicksberg theorem. □

Let us now come to the decoupled scheme from Section 3, relying on the weakened structural assumption (10) instead of (5a). Having in mind the Yanenko-type time-discrete scheme

(11), in terms of the interpolant-notation (23), the discrete variational inequality like (25) must reads as:

$$\begin{aligned}\big\langle \mathscr{I}'\dot v_\tau + \partial_u\Phi(\overline{u}_\tau,\underline{z}_\tau) - \overline{f}_\tau, \tilde v - \dot u_\tau\big\rangle + \Psi_1(\tilde v)\\ + \big\langle \partial_z\Phi(\overline{u}_\tau,\overline{\underline{z}}_\tau) - \overline{g}_\tau, \tilde z - \dot z_\tau\big\rangle + \Psi_2(\tilde z) \ge \Psi_1(\dot u_\tau) + \Psi_2(\dot z_\tau).\end{aligned} \tag{33}$$

We further use the binomial formulas (14) and the cancellation effect in (13) and, after summation for $k = 1, ..., T/\tau$, we obtain the slightly modified equality (26), namely

$$\begin{aligned}\int_0^T \big\langle \mathscr{I}'\dot v_\tau + \partial_u\Phi(\overline{u}_\tau,\underline{z}_\tau), \dot u_\tau\big\rangle + \big\langle \partial_z\Phi(\overline{u}_\tau,\overline{\underline{z}}_\tau), \dot z_\tau\big\rangle\,\mathrm{d}t\\ = \mathscr{I}(v_\tau(T)) + \Phi(u_\tau(T), z_\tau(T)) - \mathscr{I}(v_0) - \Phi(u_0, z_0).\end{aligned} \tag{34}$$

Substituting it in into (33) integrated over I, we obtain the discrete analog of (22) like (27) but now modified as

$$\begin{aligned}\int_0^T \Psi_1(\tilde v) + \Psi_2(\tilde z) + \big\langle \mathscr{I}'\dot v_\tau + \partial_u\Phi(\overline{u}_\tau,\underline{z}_\tau) - \overline{f}_\tau, \tilde v\big\rangle + \big\langle \partial_z\Phi(\overline{u}_\tau,\overline{z}_\tau) - \overline{g}_\tau, \tilde z\big\rangle\\ + \big\langle \overline{f}_\tau, \dot u_\tau\big\rangle + \big\langle \overline{g}_\tau, \dot z_\tau\big\rangle\,\mathrm{d}t + \mathscr{I}(v_0) + \Phi(u_0, z_0)\\ \ge \mathscr{I}(v_\tau(T)) + \Phi(u_\tau(T), z_\tau(T)) + \int_0^T \Psi_1(\dot u_\tau) + \Psi_2(\dot z_\tau)\,\mathrm{d}t.\end{aligned} \tag{35}$$

The a-priori estimates (29a) can be derived as before because (7) is at disposal, while the estimates (29b) can be obtained again by comparison from (24) but modified by replacing $\partial_u\Phi(\overline{u}_\tau,\overline{\underline{z}}_\tau)$ and $\partial_z\Phi(\overline{u}_\tau,\overline{\underline{z}}_\tau)$ respectively by $\partial_u\Phi(\overline{u}_\tau,\underline{z}_\tau)$ and $\partial_z\Phi(\overline{u}_\tau,\overline{\underline{z}}_\tau)$. As these terms are now nonlinear even if Φ is smooth but only component-wise quadratic, the limit passage for $\tau \to 0$ is more difficult in comparison with Proposition 5.2. We impose general assumptions:

$$\Phi, \Psi_1, \Psi_2 \ \text{ are weakly lower-semicontinuous,} \quad \|\partial\Psi_1(\cdot)\|_{U^*} \le C(1 + \|\cdot\|_U^{p_1-1}), \tag{36a}$$

$$\partial_u\Phi : U\times Z \to U^*,\ \partial_z\Phi : U\times Z \to Z^* \ \text{ are (weak,weak)-continuous.} \tag{36b}$$

Proposition 5.3 (Numerical stability of (11) and convergence.) *Let U, H, Z, f, and g be qualified as in Proposition 5.2, let $u_0 \in U$, $v_0 \in H$, $z_0 \in Z$, let further the structural assumptions (10) with (5b,c) and the qualification (36) hold. Then all the statements of Proposition 5.2 hold.*

Sketch of the Proof. The a-priori estimates (29) work by the same way as in Proposition 5.2 by exploiting (7). Then, after selection of weakly convergent subsequences, the limit passage of (35) towards (22b) is immediate due to (36). Having proved that the limit is the weak solution, (31) works in an unchanged way and yields the strong convergence (30). □

An interesting special situations occur if some processes are much faster than the external loading or the wave speed, and can be well considered as arbitrarily fast and thus rate independent. Typically is concerns the internal variable z, and then one is to consider Ψ_2 homogeneous of degree-1 and coercive on some Banach space $X \supset Z$, cf. also [17, Sect.5.1-5.2]. Then $z \in L^\infty(I;Z) \cap \mathrm{BV}(I;X)$ and Definition 5.1 is to be modified by replacing $\int_0^T \Psi_2(\dot z)\,\mathrm{d}t$ by the total variation

$$\mathrm{Diss}_{\Psi_2}(I;z) = \sup_{0\le t_0<t_1<\ldots<t_N\le T,\ N\in\mathbb{N}} \sum_{i=1}^{N} \Psi_2\big(z(t_i) - z(t_{i-1})\big). \tag{37}$$

In particular, $\dot z$ is a X-valued measure in general. If $\dot z$ is regular, such modified definition holds also on any subinterval $[t_1,t_2]\subset I$, which is the concept of weak solution used which is, under mild qualification, equivalent to a so-called local-solution concept used in the theory of rate-independent processes, cf. [17, Proposition 3.3.5]. In case of the convexity of Φ as in Proposition 5.2 but with Ψ_2 1-homogeneous, even the uniqueness of the solution is again at disposal, cf. [17, Prop. 5.1.11].

Remark 5.4 (*Convergence of the scheme from Sect. 4.)* The convergence of the modified scheme (17), i.e.

$$\dot u_\tau=\overline{v}_\tau, \qquad u_\tau\big|_{t=0}=u_0, \tag{38a}$$
$$\mathscr{T}'\dot v_\tau+\partial\Psi_1(\dot u_\tau)+\mathfrak{D}_u\Phi(\overline{u}_\tau,\underline{u}_\tau,\underline{z}_\tau)=\overline{f}_\tau, \qquad v_\tau\big|_{t=0}=v_0, \tag{38b}$$
$$\partial\Psi_2(\dot z_\tau)+\mathfrak{D}_z\Phi(\overline{u}_\tau,\overline{z}_\tau,\underline{z}_\tau)=\overline{g}_\tau, \qquad z_\tau\big|_{t=0}=z_0, \tag{38c}$$

is to exploit again (33)–(35) but with $\mathfrak{D}_u\Phi(\overline{u}_\tau,\underline{u}_\tau,\underline{z}_\tau)$ and $\mathfrak{D}_z\Phi(\overline{u}_\tau,\overline{z}_\tau,\underline{z}_\tau)$ in place of $\partial_u\Phi(\underline{\overline{u}}_\tau,\underline{z}_\tau)$ and $\partial_z\Phi(\overline{u}_\tau,\underline{\overline{z}}_\tau)$, respectively. It needs still the continuity assumption (16c). The simplest option is to require (16c) in the (weak,weak)-topology. The weak continuity of (16c) may sometimes be inadequately strong, cf. e.g. the example (45) where the weakening of (16c) by using strong topology as far as (u,π)-variables in (45) concerns (or here as far as u-variable in $\mathfrak{D}_z\Phi$ concerns). This needs to prove the strong convergence of $\overline{u}_\tau$ still before executing possibly (31). Standardly, one can make it by assuming $\Phi(\cdot,z)$ quadratic so that $\mathfrak{D}_u\Phi(\overline{u}_\tau,\underline{u}_\tau,\underline{z}_\tau)=\partial_u\Phi(\underline{\overline{u}}_\tau,\underline{z}_\tau)$, cf. the first equality in (19), and then by testing (38b) by $\underline{\overline{u}}_\tau$ while assuming a uniform monotonicity of $\partial_u\Phi$, cf. e.g. [17, Step 2 in the proof of Theorem 5.1.2], which here does not seem to work due to the energy-conserving discretisation of the inertial term. The same difficulties apply to weakening of (36b). Fortunately, sometimes particular techniques work, cf. [22].

Remark 5.5 (*Numerical implementation.)* Often, the potentials Ψ's are sum of quadratic functions with degree-1 homogeneous functions, and are then nonsmooth at 0. The qualification (5) or (10) then ensures that the minimization problems in (4) or in (12) have, after possibly a Mosco-type transformation, a structure of *Quadratic-Programming* problems (QP) if Ψ's have polyhedral epigraph (as e.g. in damage after space discretisation) or Second-Order Cone Programming (SOCP) if Ψ's have epigraphs of a so-called ice-cream-cone type (as e.g. in plasticity), cf. [17, Sect. 3.6.3] or [25, Sect. 5]. Both for QP and for SOCP, efficient algorithms and even prefabricated software packages do exist, cf. e.g. [10] and [1, 29], respectively.

6 APPLICATION IN CONTINUUM MECHANICS OF SOLIDS

The approaches from Sections 2 and 3 can be combined. We will illustrate it by considering $z=(\pi,\zeta)\in Z:=Z_1\times Z_2$ so that one can thus consider, in view of Remarks 2.1 and 3.1, the dissipation potentials $\Psi_1:Z_2\times(U\times Z_1)\to\mathbb{R}\cup\{\infty\}$ and $\Psi_2:Z_2\to\mathbb{R}\cup\{\infty\}$ and the system

$$\mathscr{T}'\,\dot u+\partial_{\dot u}\Psi_1(\zeta;\dot u,\dot\pi)+\partial_u\Phi(u,\pi,\zeta)\ni f, \qquad u|_{t=0}=u_0,\quad \dot u|_{t=0}=v_0, \tag{39a}$$
$$\partial_{\dot\pi}\Psi_1(\zeta;\dot u,\dot\pi)+\partial_\pi\Phi(u,\pi,\zeta)\ni g, \qquad \pi|_{t=0}=\pi_0, \tag{39b}$$
$$\partial\Psi_2(\dot\zeta)+\partial_\zeta\Phi(u,\pi,\zeta)\ni h, \qquad \zeta|_{t=0}=\pi_0, \tag{39c}$$

If Φ is quadratic in terms of (u,π) and also in ζ separately, one can devise two fractional steps first for (u,π) as in Sections 2 and second for ζ as in this Section 3. In a more general case when Φ is not quadratic in terms of ζ, the quotient $\mathfrak{D}_\zeta\Phi(u,\pi,\zeta,\tilde\zeta)$ should be used in place of $\partial_\zeta\Phi(u,\pi,\zeta)$, cf. Section 4. It results to the formula

$$\frac{u_\tau^k-u_\tau^{k-1}}{\tau}=v_\tau^{k-1/2}, \qquad u_\tau^0=u_0, \quad (40a)$$

$$\mathscr{T}'\frac{v_\tau^k-v_\tau^{k-1}}{\tau}+\partial_{\dot u}\Psi_1\Big(\zeta_\tau^{k-1};v_\tau^{k-1/2},\frac{\pi_\tau^k-\pi_\tau^{k-1}}{\tau}\Big) + \partial_u\Phi\big(u_\tau^{k-1/2},\pi_\tau^{k-1/2},\zeta_\tau^{k-1}\big)\ni f_\tau^k, \qquad v_\tau^0=v_0, \quad (40b)$$

$$\partial_{\dot\pi}\Psi_1\Big(\zeta_\tau^{k-1};v_\tau^{k-1/2},\frac{\pi_\tau^k-\pi_\tau^{k-1}}{\tau}\Big)+\partial_\pi\Phi\big(u_\tau^{k-1/2},\pi_\tau^{k-1/2},\zeta_\tau^{k-1}\big)\ni g_\tau^k, \qquad \pi_\tau^0=\pi_0, \quad (40c)$$

$$\partial\Psi_2\Big(\frac{\zeta_\tau^k-\zeta_\tau^{k-1}}{\tau}\Big)+\begin{cases}\partial_\zeta\Phi\big(u_\tau^k,\pi_\tau^k,\zeta_\tau^{k-1/2}\big)\ni h_\tau^k & \text{if } \Phi_0(u,\pi,\cdot) \text{ quadratic,}\\ \mathfrak{D}_\zeta\Phi\big(u_\tau^k,\pi_\tau^k,\zeta_\tau^k,\zeta_\tau^{k-1}\big)\ni h_\tau^k & \text{in general cases,}\end{cases} \qquad \zeta_\tau^0=\zeta_0. \quad (40d)$$

Hereafter, we illustrate it on a model for a damageable elasto-plastic body at small strains occupying a bounded Lipschitz domain $\Omega\subset\mathbb{R}^d$, $d=2$ or 3, possibly (cf. Remark 6.3) also in a surface variant. We will present a relatively general model of a linearized single-threshold plasticity with hardening in visco-elastic solid in Kelvin-Voigt rheology accompanied with damage allowed possibly for healing. The plastic threshold (so-called yield stress $\sigma_{\rm y}$) determines S as a ball with the radius $\sigma_{\rm y}$. The healing is an important phenomenon in some applications (in particular in geophysics) and particularly exploits combination with plastic slip so that healing can be realized in the permanently (plastically) deformed configuration, forgetting the original configuration, cf. also [17, Remark 5.2.24]. For readers' convenience, let us summarize the basic notation used in what follows:

u displacements	ϱ mass density
ζ damage scalar variable	γ damage (or delamination) coefficient
π plastic strain	$S\subset\mathbb{R}^{d\times d}_{\rm dev}$ elasticity domain (containing 0)
$e(u)$ small strain tensor	α pseudopotential of damage dissipation,
$\zeta_\flat$ delamination scalar variable	κ_1 plastic strain (or slip) gradient coefficient
$\pi_\flat$ surface plastic slip	κ_2 damage gradient coefficient
$\mathbb{C}$ elastic-moduli tensor	K elastic modulus of the adhesive
$\mathbb{D}$ viscous-moduli tensor	κ_0 hardening of plastic slip
$\mathbb{H}$ kinematic-hardening-moduli tensor	

Table 1. Summary of the basic notation used through Sections 6 and 7.

We denote by $\vec n$ the outward unit normal to $\partial\Omega$. We further suppose that the boundary of Ω splits as

$$\partial\Omega:=\Gamma=\Gamma_{\rm D}\cup\Gamma_{\rm N},$$

with $\Gamma_{\rm D}$ and $\Gamma_{\rm N}$ open subsets in the relative topology of $\partial\Omega$, disjoint one from each other and, up to $(d-1)$-dimensional zero measure, covering $\partial\Omega$. Later, the Dirichlet or the Neumann boundary conditions will be prescribed on $\Gamma_{\rm D}$ and $\Gamma_{\rm N}$, respectively. Considering $T>0$ a fixed time horizon, we set

$$I:=[0,T],\qquad Q:=(0,T)\times\Omega,\qquad \Sigma:=I\times\Gamma,\qquad \Sigma_{\rm D}:=I\times\Gamma_{\rm D},\qquad \Sigma_{\rm N}:=I\times\Gamma_{\rm N}.$$

Further, $\mathbb{R}^{d\times d}_{\rm sym}$ and $\mathbb{R}^{d\times d}_{\rm dev}$ will denote the set of symmetric or symmetric trace-free (= deviatoric) $(d\times d)$-matrices, respectively.

In the bulk model, the *state* is formed by the triple $q := (u, \pi, \zeta)$. The governing equation/inclusions read as:

$$\varrho\,\ddot u - \operatorname{div}\sigma_{\rm el} = f_0 \quad \text{with} \quad \sigma_{\rm el} = \gamma(\zeta)(\mathbb{D}\dot e_{\rm el} + \mathbb{C}e_{\rm el}), \qquad \text{(momentum equilibrium)} \tag{41a}$$

$$\partial\delta^*_S(\dot\pi) \ni \operatorname{dev}\sigma_{\rm el} - \mathbb{H}\pi + \kappa_1\Delta\pi \quad \text{with} \quad e_{\rm el} = e(u)-\pi, \qquad \text{(plastic flow rule)} \tag{41b}$$

$$\partial\alpha(\dot\zeta) \ni -\frac{1}{2}\gamma'(\zeta)\mathbb{C}e_{\rm el}{:}e_{\rm el} + \kappa_2\Delta\zeta, \qquad \text{(damage flow rule)} \tag{41c}$$

with δ_S the indicator function to a convex set S and δ^*_S its convex conjugate and with "dev" denoting the deviatoric part of a tensor, i.e. $\operatorname{dev}\sigma := \sigma - \operatorname{tr}\sigma/d$. Here, $[\mathbb{C}e]_{ij}$ means $\sum_{k,l=1}^d \mathbb{C}_{ijkl}e_{kl}$.

Of course, (41) is to be completed by appropriate boundary conditions, e.g.

$$u = w_{\rm D} \qquad \text{on } \Gamma_{\rm D}, \tag{42a}$$

$$\sigma_{\rm el}\cdot\vec n = f_1 \qquad \text{on } \Gamma_{\rm N}, \tag{42b}$$

$$\kappa_1\nabla\pi\vec n = 0 \quad \text{and} \quad \kappa_2\nabla\zeta\cdot\vec n = 0 \qquad \text{on } \Gamma \tag{42c}$$

with $\vec n$ denoting the unit outward normal to Ω. We will consider an initial-value problem for (41)–(42) by asking for

$$u(0) = u_0, \qquad \dot u(0) = v_0, \qquad \pi(0) = \pi_0, \quad \text{and} \quad \zeta(0) = \zeta_0. \tag{43}$$

The abstract spaces and the energy functionals used in (41) are now:

$$U = H^1(\Omega;\mathbb{R}^d), \qquad Z_1 = \begin{cases} L^2(\Omega;\mathbb{R}^{d\times d}_{\rm dev}) & \text{if } \kappa_1 = 0,\\ H^1(\Omega;\mathbb{R}^{d\times d}_{\rm dev}) & \text{if } \kappa_1 > 0,\end{cases} \qquad Z_2 = H^1(\Omega)\cap L^\infty(\Omega), \tag{44a}$$

$$\Phi(u,\pi,\zeta) = \int_\Omega \frac{1}{2}\gamma(\zeta)\mathbb{C}(e(u)-\pi){:}(e(u)-\pi) + \frac{1}{2}\mathbb{H}\pi{:}\pi + \frac{\kappa_1}{2}|\nabla\pi|^2 + \frac{\kappa_2}{2}|\nabla\zeta|^2\,{\rm d}x, \tag{44b}$$

$$\Psi_1(\zeta;\dot u,\dot\pi) = \int_\Omega \frac{1}{2}\gamma(\zeta)\mathbb{D}(e(\dot u)-\dot\pi){:}(e(\dot u)-\dot\pi) + \delta^*_S(\dot\pi)\,{\rm d}x, \qquad \Psi_2(\dot\zeta) = \int_\Omega \alpha(\dot\zeta)\,{\rm d}x, \tag{44c}$$

$$\mathscr{T}(\dot u) = \int_\Omega \frac{\varrho}{2}|\dot u|^2\,{\rm d}x, \qquad \big\langle f(t), u\big\rangle = \int_\Omega f_0(t,\cdot)\cdot u\,{\rm d}x + \int_{\Gamma_{\rm N}} f_1(t,\cdot)\cdot u\,{\rm d}S, \tag{44d}$$

with $\mathbb{C}$ and $\mathbb{D}$ positive-definite 4th-order tensors, $\mathbb{H}$ a positive-definite 4th-order tensor, $\alpha : \mathbb{R}\to[0,\infty]$ convex with $\alpha(0) = 0$, and $\kappa_1 \ge 0$ and $\kappa_2 > 0$ given coefficients. Furthermore, $\gamma : \mathbb{R}\to\mathbb{R}^+$ is positive (i.e. allowing only for an incomplete damage) continuously differentiable nondecreasing with $\gamma' = 0$ on $(-\infty,0]\cup[1,\infty)$, which ensures that the values of ζ ranges the interval $[0,1]$ if ζ_0 do so.

Written in the classical formulation, the differential quotient used in (40d) can be now taken as

$$\mathfrak{D}_\zeta\Phi\big(u,\pi,\zeta,\tilde\zeta\big) := \begin{cases} \dfrac{1}{2}\dfrac{\gamma(\zeta)-\gamma(\tilde\zeta)}{\zeta-\tilde\zeta}\mathbb{C}(e(u)-\pi){:}(e(u)-\pi) & \\ \qquad\qquad -\dfrac{1}{2}\kappa_2\Delta\zeta - \dfrac{1}{2}\kappa_2\Delta\tilde\zeta & \text{on } \{x\in\Omega;\ \zeta(x)\ne\tilde\zeta(x)\},\\ \dfrac{1}{2}\gamma'(\zeta)\mathbb{C}(e(u)-\pi){:}(e(u)-\pi) - \kappa_2\Delta\zeta & \text{on } \{x\in\Omega;\ \zeta(x)=\tilde\zeta(x)\}.\end{cases} \tag{45}$$

Note that it obviously satisfies (16a,b). Moreover, the assumption (16c) holds in the variant of the (strong×weak×weak×weak,weak*)-continuity since $\gamma(\cdot)$ is assumed continuously differentiable with γ' bounded and $\kappa_2 > 0$ so that we can use Rellich compact-embedding theorem for ζ and $\tilde\zeta$. This needs to prove strong convergence of $\overline{u}_\tau$ mentioned in Remark 5.4. This may be quite technical. Here, it holds for a special case that $\mathbb{D} = \chi\mathbb{C}$ for some relaxation time $\chi > 0$, see [22, Step 3 in the proof of Prop. 4]. Also (16e) holds with the potential $\mathfrak{G}_{u,\pi,\tilde\zeta}$ given by

$$\mathfrak{G}_{u,\pi,\tilde\zeta}(\zeta) = \int_\Omega \left(\frac{\kappa_2}{4}|\nabla\zeta|^2 + \frac{1}{2}\mathbb{C}(e(u(x))-\pi(x)):(e(u(x))-\pi(x)) \int_0^{\zeta(x)} \Gamma_{\tilde\zeta(x)}(z)\,\mathrm{d}z \right)\mathrm{d}x$$
$$\text{with} \quad \Gamma_{\tilde z}(z) = \begin{cases} (\gamma(z)-\gamma(\tilde z))/(z-\tilde z) & \text{if } z \neq \tilde z, \\ \gamma'(z) & \text{if } z = \tilde z. \end{cases} \tag{46}$$

For the time discretisation (40), one considers the structure (39) and use the Crank-Nicolson scheme for displacement with plasticity together and then backward Euler discretization for damage. It results to the formula (40). Note that coupling of $\dot u$ and $\dot\pi$ in the dissipation potential Ψ_1 in (44) allows for considering the viscous dissipation acting more physically on the elastic strain $e(u)-\pi$ instead on the total strain $e(u)$ and the plastic strain π separately.

Remark 6.1 (*Ambrosio-Tortorelli's approximation of cracks.)* The standard case of rate-independent first-order damage gradient can be applied in the energy-conserving Yanenko scheme when a cohesive damage which does not need the constraint $\zeta \geq 0$ is considered. This situation occurs if $\gamma'(0) = 0$. In particularly, it holds for $\gamma(\zeta) = \epsilon + \zeta^2$ with $\epsilon > 0$ which occurs in particular in the so-called Ambrosio-Tortorelli approximation [2] of the fracture, rigorously devised in the static scalar case and then suggested also for the dynamical situation in [17, Sect. 5.2.5] without guaranteeing any convergence towards the brittle fracture in the visco-elastic bulk, however. Keeping ζ valued in $[0,1]$ can then be made by considering $\alpha([0,\infty)) = \infty$ so that no healing is allowed. The analysis of the energy-conserving scheme from Sect. 3 even coupled with diffusion is in [22].

Remark 6.2 (*Polycrystalic shape-memory alloys.)* Another noteworthy component-wise quadratic model for phase-transformations in shape-memory materials which considers $e_{\rm el} = e(u) - \lambda\pi_{\rm tr}$ in (44) with $0 \leq \lambda \leq 1$ a volume fraction between so-called austenite and martensite, and $\pi_{\rm tr}$ a transformation strain that is subjected to a constraint on its magnitude. Cf. the polycrystalic models in [4, 26] possibly also in combination with plasticity like already used in (44) with a decoupled dissipation similarly like in (39). A suitable transformation allows more coupled dissipation, cf. [13, 27], and then, after penalization of the constraints, a one-step formula as used in Sect. 2 but modified as in Sect. 4.

Remark 6.3 (*Surface plasticity and damage.)* Considering a contact interface $\Gamma_{\rm C}$ as a part of the boundary of Ω, a useful surface analog of the bulk model exploits as the internal variables a surface *plastic slip* $\pi_\flat : \Gamma_{\rm C} \to \mathbb{R}^{d-1}$ as in [23, 24] and a surface damage (also called a *delamination* parameter) $\zeta_\flat : \Gamma_{\rm C} \to [0,1] \subset \mathbb{R}$ as invented by Frémond [12]. A combination with the plastic slip was devised in [23, 24] to model a mode-mixity dependent delamination, reflecting the phenomenon that the Mode II (shear) needs/dissipates usually considerably more energy to delaminate than Mode I (opening). Advantageously, compactness of the

trace operator $u \mapsto u|_{\Gamma_C}$ simplifies some analytical aspects. In the case of a so-called normal-compliance adhesive contact (with the compliance described by a function $p(\cdot)$), the classical formulation of such problem consists in the equilibrium of forces on the domain Ω with the boundary condition on $\Gamma_N = \Gamma\backslash\Gamma_C$ and several complementarity problems on the contact boundary Γ_C. In the Kelvin-Voigt rheology, the model looks as:

$$\begin{aligned}
&\dot u = v, \qquad \varrho\dot v - \operatorname{div}\sigma = 0, \qquad \sigma = \mathbb{C}e(u) + \mathbb{D}e(v), && \text{in } \Omega, && (47a)\\
&\sigma\nu = f_1(t) && \text{on } \Gamma, && (47b)\\
&\left.\begin{aligned}
&\sigma_n + \gamma(\zeta_\flat)Ku_n + p(u_n) = 0, \qquad \sigma_t = \gamma(\zeta_\flat)K(u_t - \pi_\flat),\\
&\partial\delta_S^*(\dot\pi_\flat) \ni \sigma_t - \kappa_0\pi_\flat + \operatorname{div}_S(\kappa_1\nabla_S\pi_\flat),\\
&\partial\alpha(\dot\zeta_\flat) \ni -\tfrac12\gamma'(\zeta_\flat)K|u_t - \pi_\flat|^2 + \operatorname{div}_S(\kappa_2\nabla_S\zeta_\flat),
\end{aligned}\right\} && \text{on } \Gamma_C, && (47c)
\end{aligned}$$

where η is the driving "force" for the plastic-slip evolution, $\sigma\nu := (\mathbb{C}e(u)+\mathbb{D}e(v))\big|_\Gamma\nu$ is the traction stress on $\Gamma = \Gamma_C$ or Γ_N. Moreover, its normal and tangential components on Γ_C are denoted with $\sigma_n(u) = (\sigma\nu)\cdot\nu$ and $\sigma_t(u) = \sigma\nu - ((\sigma\nu)\cdot\nu)\nu$, respectively, so that we have the decomposition $\sigma\nu = \sigma_n\nu + \sigma_t$. In (47c), $\operatorname{div}_S := \operatorname{trace}(\nabla_S)$ denotes the $(d-1)$-dimensional "surface divergence" and ∇_S a "surface gradient", i.e. the tangential derivative defined as $\nabla_S v = \nabla v - (\nabla v\cdot\nu)\nu$ for v defined on Γ_C. Actually, we assume here that Γ_C is flat, otherwise also a curvature term like $(\operatorname{div}_S\nu)(\kappa\nabla_S\pi_\flat\nu)$ should contribute to the corresponding driving force η. This problem has a structure (39) if the stored-energy, the kinetic-energy, and the dissipation functionals and the loading are set now as:

$$\begin{aligned}
\Phi(u,\pi_\flat,\zeta_\flat) = \int_\Omega \frac12\mathbb{C}e(u){:}e(u)\,\mathrm{d}x + \int_{\Gamma_C}\frac12\gamma(\zeta_\flat)K\big(u_n^2 + |u_t-\pi_\flat|^2\big) + \widehat p(u_n)\\
+ \frac{\kappa_0}{2}|\pi_\flat|^2 + \frac{\kappa_1}{2}|\nabla_S\pi_\flat|^2 + \frac{\kappa_2}{2}|\nabla_S\zeta_\flat|^2\,\mathrm{d}S, && (48a)
\end{aligned}$$

$$\Psi_1(\dot u,\dot\pi_\flat) = \int_\Omega\frac12\mathbb{D}e(\dot u){:}e(\dot u)\,\mathrm{d}x + \int_{\Gamma_C}\delta_S^*(\dot\pi_\flat)\,\mathrm{d}S, \qquad \Psi_2(\dot\zeta_\flat) = \int_{\Gamma_C}\alpha(\dot\zeta_\flat)\,\mathrm{d}S, \tag{48b}$$

$$\mathscr{T}(\dot u) = \int_\Omega\frac{\varrho}{2}|\dot u|^2\,\mathrm{d}x, \qquad \big\langle f(t),u\big\rangle = \int_\Gamma f_1(t,\cdot)\cdot u\,\mathrm{d}S, \tag{48c}$$

with $\widehat p$ a primitive function to p. The underlying Banach spaces are taken as

$$U = H^1(\Omega;\mathbb{R}^d), \qquad Z_1 = \begin{cases} L^2(\Gamma_C;\mathbb{R}^{d-1}) & \text{if } \kappa_1 = 0,\\ H^1(\Gamma_C;\mathbb{R}^{d-1}) & \text{if } \kappa_1 > 0,\end{cases} \qquad Z_2 = L^\infty(\Gamma_C). \tag{48d}$$

If $[\zeta_\flat]_0 \in [0,1]$ on Γ_C (as usually assumed), then $\zeta_\flat$ remains valued in $[0,1]$ during the whole evolution provided $\gamma(\cdot)$ is qualified as before. Now we can easily afford the complete surface damage (delamination), i.e. $\gamma(\zeta) = 0$ if $\zeta \le 0$.

Remark 6.4 (*Stress formulation, Maxwell/Jeffreys rheology.)* A modification of the original 1st-order system (47a) by elimination of u-variable leads to a stress/velocity formulation

$$\mathbb{C}^{-1}\dot\sigma = e(v) + \mathbb{C}^{-1}\mathbb{D}e(\dot v) \qquad \& \qquad \varrho\dot v - \operatorname{div}\sigma = 0. \tag{49}$$

This allows for a combination with the so-called mixed FEM, cf. [5] for the case $\mathbb{D} = 0$. It further allows for a straightforward modification by adding the terms $\mathbb{D}_{\text{Max}}^{-1}\sigma$ and $\mathbb{D}_{\text{Max}}^{-1}\mathbb{D}e(v)$:

$$\mathbb{C}^{-1}\dot\sigma + \mathbb{D}_{\text{Max}}^{-1}\sigma = (\mathbb{I}+\mathbb{D}_{\text{Max}}^{-1}\mathbb{D})e(v) + \mathbb{C}^{-1}\mathbb{D}e(\dot v) \qquad \& \qquad \varrho\dot v - \operatorname{div}\sigma = 0$$

with $\mathbb{D}_{\rm Max}$ another viscous-moduli tensor. For $\mathbb{D}=0$ and $\mathbb{D}_{\rm Max}>0$ we thus obtain the Maxwell rheology while for $\mathbb{D}>0$ and $\mathbb{D}_{\rm Max}>0$ such rheological model is called the Jeffreys material as a Norton-Hoff (Stokes) and a Maxwell rheologies in parallel. For $\mathbb{D}_{\rm Max}\to\infty$ we obtain the Kelvin-Voigt model (49). Both are fluids in the sense that they cannot permanently withstand stress under a bounded strain response. Creep effects can thus be modeled. After being discretised by Crank-Nicolson scheme, it looks as:

$$\begin{aligned}&\varrho\tfrac{v_\tau^k-v_\tau^{k-1}}{\tau}-\operatorname{div}\sigma_\tau^{k-1/2}=0,\\&\mathbb{C}^{-1}\tfrac{\sigma_\tau^k-\sigma_\tau^{k-1}}{\tau}+\mathbb{D}_{\rm Max}^{-1}\sigma_\tau^{k-1/2}=(\mathbb{I}+\mathbb{D}_{\rm Max}^{-1}\mathbb{D})e\big(v_\tau^{k-1/2}\big)+\mathbb{C}^{-1}\mathbb{D}e\Big(\tfrac{v_\tau^k-v_\tau^{k-1}}{\tau}\Big).\end{aligned}$$

To reveal the energetics, we express $e(v_\tau^{k-1/2})=\mathbb{C}^{-1}(\frac{\sigma_\tau^k-\sigma_\tau^{k-1}}{\tau}-\mathbb{D}e(\frac{v_\tau^k-v_\tau^{k-1}}{\tau}))+\mathbb{D}_{\rm Max}^{-1}(\sigma_\tau^{k-1/2}-\mathbb{D}e(v_\tau^{k-1/2})$ and test it by $\sigma_\tau^{k-1/2}-\mathbb{D}e(v_\tau^{k-1/2})$. After using several binomial formulas similarly as before, we obtain the discrete energy balance (as an equality):

$$\begin{aligned}\frac{1}{\tau}\bigg(\int_\Omega\frac{1}{2}\mathbb{C}^{-1}(\sigma_\tau^k-\mathbb{D}e(v_\tau^k)):(\sigma_\tau^k-\mathbb{D}e(v_\tau^k))-\frac{1}{2}\mathbb{C}^{-1}(\sigma_\tau^{k-1}-\mathbb{D}e(v_\tau^{k-1})):(\sigma_\tau^{k-1}-\mathbb{D}e(v_\tau^{k-1}))\,{\rm d}x\bigg)\\+\int_\Omega\mathbb{D}e(v_\tau^{k-1/2}):e(v_\tau^{k-1/2})+\mathbb{D}_{\rm Max}^{-1}(\sigma_\tau^{k-1/2}-\mathbb{D}e(v_\tau^{k-1/2})):(\sigma_\tau^{k-1/2}-\mathbb{D}e(v_\tau^{k-1/2}))\,{\rm d}x\\=\int_\Omega f_\tau^k\cdot v_\tau^k\,{\rm d}x+\int_\Gamma g_\tau^k\cdot v_\tau^k\,{\rm d}S.\end{aligned}$$

7 ILLUSTRATIVE COMPUTATIONAL SIMULATIONS

We illustrate the above sections on a Mode-II frictional-type or adhesive contact problem from Remark 6.3. All these inelastic process occurs only on (a part) of the boundary, let us denote it by $\Gamma_{\rm C}$. The resting part of the boundary will be denoted by $\Gamma_{\rm N}$ and part of it, denoted by $\Gamma_{\rm N1}$, will be loaded by time-dependent force.

The time-discretisation scheme (40) has been used. In particular, it complies with the energy conservation at all time intervals when the delamination $\zeta_\flat$ does not evolve. The space-discretisation was performed by FEM, namely by using the Q1-elements for u and P0-elements for both $\pi_\flat$ and $\zeta_\flat$ on the boundary $\Gamma_{\rm C}$. For the special case where $\mathbb{D}{=}\chi\mathbb{C}$, with χ a given relaxation time, damping matrix may be defined as proportional to stiffness, that is a special case for the device known as Rayleigh damping [8]. Here we exploited that we consider only such particular cases which do not require gradient of $\pi_\flat$ i.e. both $\kappa=0$ can be used for the two experiments below because they consider only either the plastic slip or the delamination, but not their combination, cf. also Remark 7.2.

The isotropic viscoelastic material of the bulk is aluminum with the Young modulus $E=70$GPa, Poisson ratio $\nu=0.35$, i.e. $\mathbb{C}_{ijkl}\doteq[60\delta_{ij}\delta_{kl}+26(\delta_{ik}\delta_{jl}{+}\delta_{il}\delta_{jk})]$GPa, and mass density $\varrho=2700\,{\rm kg/m^3}$. Elastic plain strain is considered for 2-dimensional computational experiments. Moreover, we consider a Mode-II contact in the sense that $u_{\rm n}=0$ on $\Gamma_{\rm C}$, which means sending the compliance slope $p(\cdot)$ in (47c) to infinity. Rather formally, we consider a very small viscosity $\mathbb{D}=\chi\mathbb{C}$ with $\chi=2\,{\rm ns}$ implemented simply as in [19] to comply with our convergence-analysis arguments, although it does not have visible effects in our simulations. We also do not consider hardening, i.e. $\kappa_0=0$ in (48a); in fact, the coercivity of Φ in terms

of $\pi_\flat$ is then ensured through the coercivity of u_t by cooperation of Korn's inequality and inertia if $\inf\gamma(\cdot)>0$ or through the coercivity of α in (48b) with $\kappa_1>0$, which is applicable in Sections 7.1 and 7.2.

We perform our illustrative computational experiments for $d=2$, using a rectangular 2-dimensional domain Ω in Figs. 1 and 5. For the spatial discretisation, Ω was divided into 2×40=80 squares for the coarsest spacial discretisation, and then also refined 4 and 9 times for 320 and 720 square elements.

7.1 Frictional-contact experiment without adhesion

As a particular situation, we send α to infinity which practically means that $\dot\zeta_\flat=0$ and $\zeta_\flat$ stays constant during the whole evolution, say $\zeta_\flat=[\zeta_\flat]_0\equiv1$. In other words, we just omit $\zeta_\flat$ here. Further modeling ansatz is to consider K large on Γ_C, namely $K=75\,\mathrm{GPa/m}$. This causes that the difference $u_\mathrm{t}-\pi_\flat$ is small during the whole evolution and we can recognize the model as a regularized dry-friction model with σ_y playing a role of the friction coefficient, cf. also [17, Remark 5.2.17]. More specifically, it is a so-called given friction (also called Tresca's friction) which neglects influence of possible variation of the normal force on the tangential friction. To show influence of the friction, two values of the yield stress determining the

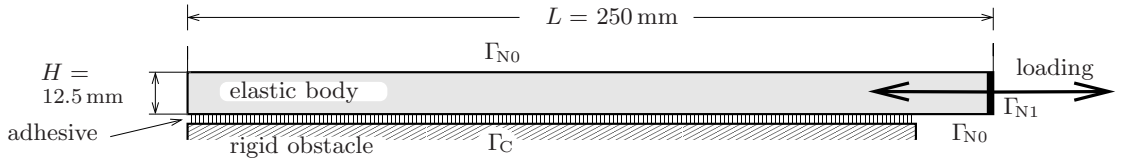

Figure 1: *Geometry of a 2-dimensional rectangular-shaped specimens subjected to a cyclically loading $f_1=f_1(t)$ the right-hand side $\Gamma_{\mathrm{N}1}$.*

sliding resistance (i.e. the prescribed Tresca friction) has been chosen, namely $\sigma_\mathrm{y}=3\,\mathrm{MPa}$ and 6 MPa, referred respectively as "small" and "large" friction in Figures 2–4. We consider a 2-dimensional rectangular specimen, cf. Fig. 1. The adhesive part Γ_C is considered to be that of 0.9 of the total length, cf. again Fig. 1.

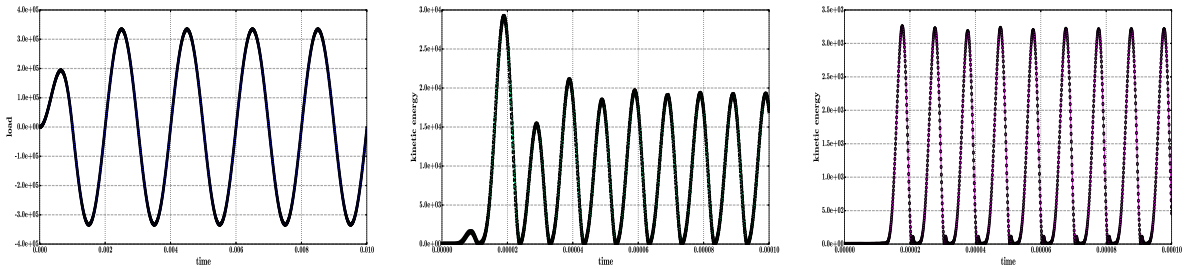

given load **small friction** **large friction**

Figure 2: *Computational results of the frictional-contact experiment from Fig. 1:*
Left: the prescribed cycling force loading $f_1=f_1(t)$.
Middle/Right: the kinetic energy for all of the three meshes used for calculations (differences practically invisible) for two friction coefficients.

The one-step Crank-Nicolson scheme from Sect. 2 is used. The coarsest time discretisation

used 500 time steps, for total time of the experiment that of 1 ms, and then we compare it also for a twice and three-times finer time discretisation when refining simultaneously the space discretisation.

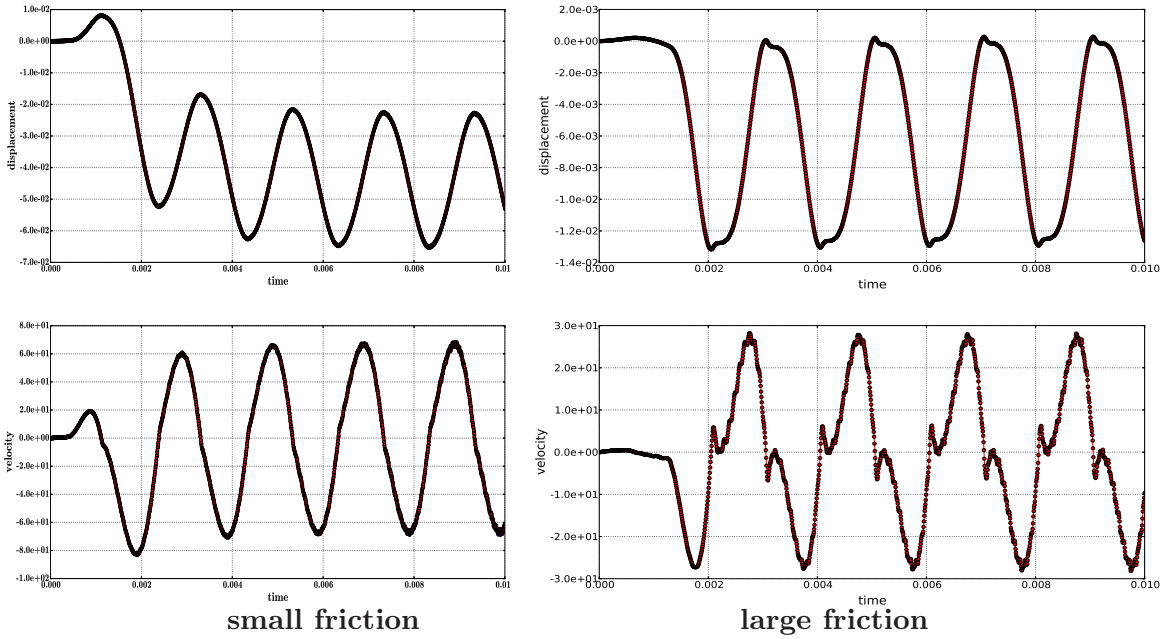

Figure 3: *The displacement (upper diagrammes) at the right-hand end of the bar from Fig. 1 and its time derivative, i.e. the velocity (lower diagrammes). The oscillatory behaviour clearly demonstrates the role of inertia preventing the immediate blow up after the sliding resistence due to friction is first overcome. In addition, high-frequency vibrations in eigen modes of the bar are visible under large friction (i.e. in the right-hand collum).*

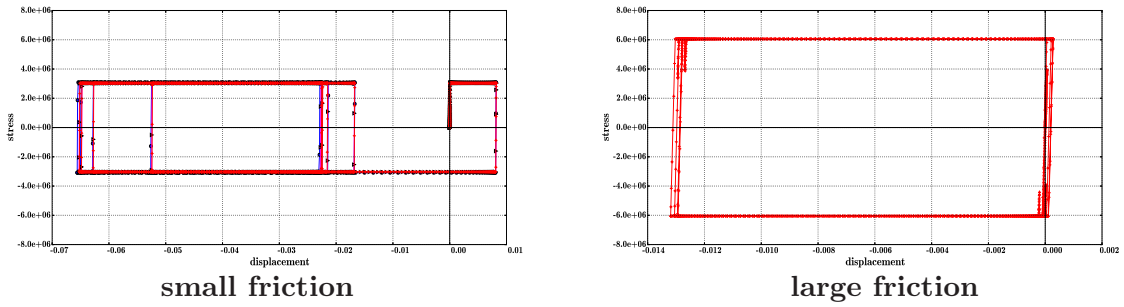

Figure 4: *Typical clock-wise (so-called stop-operator) hysteretic loop in the graph displacement versus stress.*

On the right-hand side Γ_{N1} of the specimen we assume a cyclic loading in time as depicted in the left plot of Fig. 2-left. Numerical convergence is documented by the plots in Fig. 2-middle/right. The computed response on the free right-hand side of the bar is depicted in plots of Fig. 3 both for displacement (left) and velocity (right). In order to check algorithmic performance reults of all the three meshes considered are shown on the same plots. Finally a typical hysteresis loop in the graph displacement versus stress for a material point of the adhesive interface part is shown in Fig. 4, once again results obtained for all the three considered meshes are given there. The presence of inertia is essential otherwise the coercivity under the mere force loading without any hardening would be lost and instead of an oscillating transient response on Figure 3, we would see an instantaneous blow-up at time when the friction threshold is reached.

7.2 Delamination experiment

The geometry is similar to the previous example except that we now consider the adhesive contact only on a smaller part of the bottom side (namely 1/10 of the total length of the specimen, cf. Fig. 5, and a monotonically increasing loading on the right-hand side up to a complete-rupture time (about 0.7 s) after which it drops to zero. The material of the bar as well as of the adhesive is the same as in the previous example from Sect. 7.1, except of the fact that in this case we assume Mode-II fracture toughness to have the value $a_2 = 187.5$ J/m^2, while we send σ_y to infinity which practically means that $\dot{\pi}_\flat = 0$ and thus, putting also $\pi_\flat|_{t=0} = 0$, the plasticity has been supressed in this experiment.

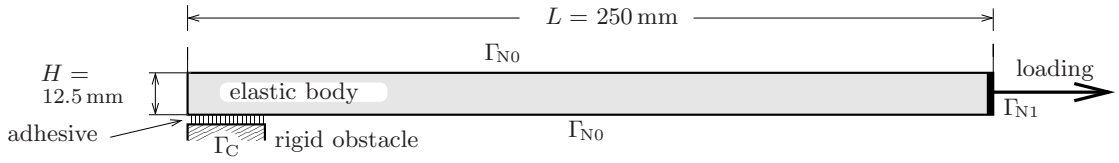

Figure 5: *Geometry of a 2-dimensional rectangular-shaped specimens subjected to the monotonically increasing loading $f_1 = f_1(t)$ on the right-hand side Γ_{N1}.*

This experiment wants to show emission of an elastic wave during sudden rupture of the adhesive contact. The fractional-step (with two steps) Crank-Nicolson scheme from Sect. 3 is used. In this case the coarsest time discretisation used 5000 time steps, for total time of the experiment that of 5 sec, and then we compare it also for a twice and three-times finer time discretisation when refining also the space discretisation.

Furthermore, distinguishing energies of the system may be seen in the plot of Fig. 6-left, where more specific elastic, kinetic together with the adhesive stored energy, due to damage dissipation and the damping are shown. Moreover, velocity of the right-hand side of the domain, as computed using all the three meshes, is depicted in Fig. 6-right. Finally, velocity of the left-most bottom point is depicted in Fig. 7-left. Result are given for all the meshes, while in plot of Fig. 7-right, results computed using the finer mesh are given for sequentially point on the adhesive. It might observed there the sequence of damage evolution and furth motion after that.

Remark 7.1 (*Handling the constraint $\zeta_\flat \geq 0$.*) A more conventional handling of the constraint $\zeta_\flat \geq 0$ is to implement it as a variational inequality and then one can consider $A(\cdot)$

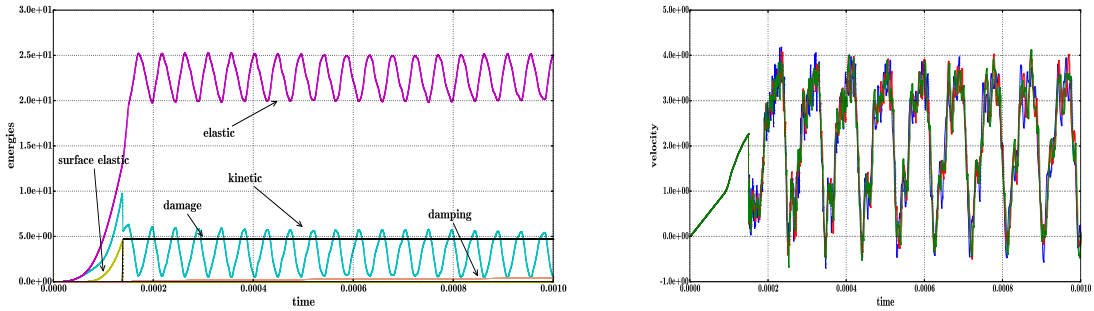

Figure 6: *Results of the delamination experiment from Fig. 5:*
Left: time evolution of energies of the system showing in particular non-attenuated oscillations of kinetic and elastic energies after rupture at time $t \doteq 0.14\,\mathrm{ms}$.
Right: computed velocity of the right-hand side of the domain. The high-frequency vibrations are superposed to the oscillation of the bar on the lowest eigen-frequence.

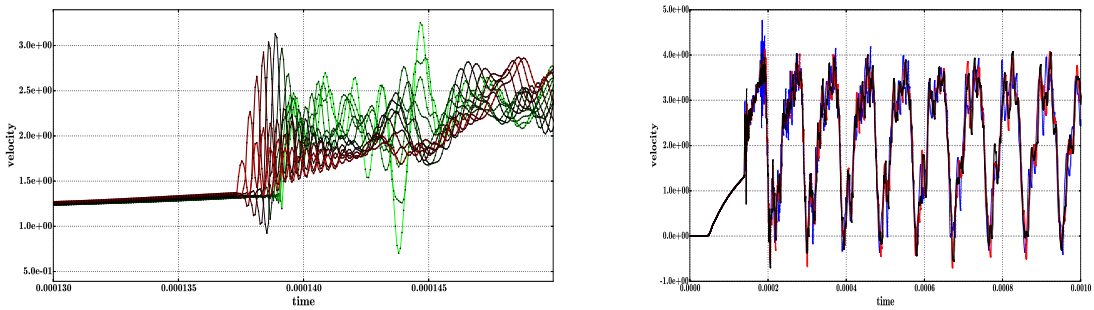

Figure 7: *Results of the delamination experiment from Fig. 5:*
Left: A detail of damage evolution on the time interval $[0.13\,\mathrm{ms}, 0.15\,\mathrm{ms}]$ *around the rupture time tracking the velocity at particular mesh points on the adhesive.*
Right: velocity like in Fig. 6-right but on the left-hand side of the specimen from Fig. 5.

linear to model a standard adhesive delamination. We can obtain it only as a limit from our model Noteworthy, this variational-inequality limit problem is not compatible with our energy-conserving discretisation, although the discretisation of all the approximate problems exactly conserves energy. In fact, for simplicity, the calculations presented in this Section 7.2 have been performed by this variational-inequality limit problem, the violation of energy conservation only during the short time interval of rupture having been practically invisible below 0.1%.

Remark 7.2 (*Combination of damage and plasticity.)* One can combine both inelastic processes like in the bulk model mentioned in Section 6. One would then deal with the model from [23,24] originally considered in quasistatic variant and devised to distinguish Mode I and Mode II delamination. Here we considered intentionally only Mode II otherwise one should rather consider a unilateral contact which would then be incompatible with our assumption of Φ being quadratic in terms of u. Here $\kappa > 0$ is needed to facilitate the analysis.

Acknowledgments: This research was supported from the grants 14-15264S "Experimentally justified multiscale modelling of shape memory alloys" and 16-03823S "Homogenization and multi-scale

computational modelling of flow and nonlinear interactions in porous smart structures" of the Czech Science Foundation, and from the institutional support RVO: 61388998 (ČR).

References

[1] F. Alizadeh and D. Goldfarb. Second-order cone programming. *Math. Program., Ser. B*, 95:3–51, 2003.

[2] L. Ambrosio and V. M. Tortorelli. Approximation of functional depending on jumps via by elliptic functionals via Γ-convergence. *Comm. Pure Appl. Math.*, 43:999–1036, 1990.

[3] F. Armero and E. Petötz. Formulation and analysis of conserving algorithms for dynamic contact/impact problems. *Computer Meth. Appl. Mech. Engr.*, 158:269–300, 1998.

[4] F. Auricchio, A. Reali, and U. Stefanelli. A three-dimensional model describing stress-induced solid phase transformation with permanent inelasticity. *Int. J. Plasticity*, 23:207–226, 2007.

[5] E. Bécache, P. Joly, and C. Tsogka. A new family of mixed finite elements for the linear elastodynamic problem. *SIAM J. Numer. Anal.*, 39:2109–2132, 2002.

[6] J. Chung and G. M. Hulbert. A time integration algorithm for structural dynamics with improved numerical dissipation: the generalized-α method. *J. Appl. Mech.*, 60:371–375, 1993.

[7] N. Condette, C. Melcher, and E. Süli. Spectral approximation of pattern-forming nonlinear evolution equations with double-well potentials of quadratic growth. *Math. Comput.*, 80:205–223, 2011.

[8] R. D. Cook, D. S. Malkus, M. E. Plesha, and R. J. Witt. *Concepts and Applications of Finite Element Analysis*. Wiley, 2001.

[9] J. Crank and P. Nicolson. A practical method for numerical evaluation of solutions of partial differential equations of the heat conduction type. *Proc. Camb. Phil. Soc.*, 43:50–67, 1947.

[10] Z. Dostál. *Optimal Quadratic Programming Algorithms*. Springer, Berlin, 2009.

[11] I. Faragó. Splitting methods and their application to the abstract Cauchy problems. Lect. Notes Comp.Sci. 3401, pages 35–45. Springer, Berlin, 2005.

[12] M. Frémond. Dissipation dans l'adhrence des solides. *C. R. Acad. Sci., Paris, Sér.II*, 300:709–714, 1985.

[13] M. Frost, B. Benešová, and P. Sedlák. A microscopically motivated constitutive model for shape memory alloys: formulation, analysis and computations. *Math. Mech. of Solids*, 21:358–382, 2016.

[14] R. Glowinski, J.-L. Lions, and R. Trémolières. *Numerical analysis of variational inequalities*. North-Holland, Amsterdam, 1981. (French original Dunod, Paris, 1976).

[15] H. M. Hilber, T. J. R. Hughes, and R. L. Taylor. Improved numerical dissipation for time integration algorithms in structural dynamics. *Earthquake Eng. Struct. Dyn.*, 5:283–292, 1977.

[16] G. Marchuk. *Splitting and Alternating Direction Methods*. North Holland, Amsterdam, 1990.

[17] A. Mielke and T. Roubíček. *Rate-Independent Systems – Theory and Application*. Springer, New York, 2015.

[18] N. M. Newmark. A method of computation for structural dynamics. *J. Eng. Mech. Div.*, 85:67–94, 1959.

[19] C. G. Panagiotopoulos, V. Mantič, and T. Roubíček. A simple and efficient BEM implementation of quasistatic linear visco-elasticity. *Intl. J. Solids Structures*, 51:2261–2271, 2014.

[20] E. Paraskevopoulos, C. Panagiotopoulos, and D. Talaslidis. Rational derivation of conserving time integration schemes: the moving-mass case. In M. Papadrakakis et al., editor, *Computational Structural Dynamics and Earthquake Engineering*, chapter 10, pages 149–164. CRC Press, Bocca Raton, 2009.

[21] T. Roubíček. *Nonlinear Partial Differential Equations with Applications*. Birkhäuser, Basel, 2nd edition, 2013.

[22] T. Roubíček. Energy-conserving time-discretisation scheme for poroelastic media with regularized fracture emitting waves and heat. *Discr. Cont. Dynam. Systems Ser. S*, to appear.

[23] T. Roubíček, M. Kružík, and J. Zeman. Delamination and adhesive contact models and their mathematical analysis and numerical treatment. In V. Mantič, editor, *Math. Methods & Models in Composites*, chapter 9, pages 349–400. Imperial College Press, 2013.

[24] T. Roubíček, V. Mantič, and C. G. Panagiotopoulos. Quasistatic mixed-mode delamination model. *Discr. Cont. Dynam. Systems Ser. S*, 6:591–610, 2013.

[25] T. Roubíček and J. Valdman. Stress-driven solution to rate-independent damage with plasticity at small strains and its computer implementation. *Math. Mech. Solids*, in print. DOI: 10.1177/1081286515627674.

[26] A. Sadjadpour and K. Bhattacharya. A micromechanics inspired constitutive model for shape-memory alloys. *Smart Mater. Structures*, 16:1751–1765, 2007.

[27] P. Sedlák, M. Frost, B. Benešová, T. Ben Zineb, and P. Šittner. Thermomechanical model for NiTi-based shape memory alloys including R-phase and material anisotropy under multi-axial loadings. *Intl. J. Plasticity*, 39:132–151, 2012.

[28] J. C. Simo and J. R. Hughes. *Computational Inelasticity*. Springer, Berlin, 1998.

[29] J. F. Sturm. Implementation of interior point methods for mixed semidefinite and second order cone optimization problems. *Optim. Meth. Software*, 17:1105–1154, 2002.

[30] L. Wang. *Foundations of Stress Waves*. Elsevier, Amsterdam, 2007.

[31] L. C. Wellford Jr. and S. M. Hamdan. An analysis of the stability and convergence properties of a Crank-Nicholson algorithm for nonlinear elasto-dynamics problems. In W. Wunderlich, E. Stein, and K.-J. Bathe, editors, *Nonlinear Finite Element Analysis in Structural Mechanics*, pages 502–518, Berlin, 1981. Springer.

[32] N. N. Yanenko. *The Method of Fractional Steps*. Springer, Berlin, 1971.

[33] O. C. Zienkiewicz, W. L. Wood, N. W. Hine, and R. L. Taylor. A unified set of single step algorithms. Part 1: General formulation and applications. *Intl. J. Numer. Meth. Engr.*, 20:1529–1552, 1984.